Bounds of Asymptotic Performance Limits of Social-Proximity Vehicular Networks

Ning Lu, *Student Member, IEEE*, Tom H. Luan, Miao Wang, Xuemin Shen, *Fellow, IEEE*, and Fan Bai

***Abstract*—In this paper, we investigate the asymptotic performance limits (throughput capacity and average packet delay) of social-proximity vehicular networks. The considered network involves N vehicles moving and communicating on a scalable grid-like street layout following the social-proximity model: Each vehicle has a restricted mobility region around a specific social spot and transmits via a unicast flow to a destination vehicle that is associated with the same social spot. Moreover, the spatial distribution of the vehicle decays following a power-law distribution from the central social spot toward the border of the mobility region. With vehicles communicating using a variant of the two-hop relay scheme, the asymptotic bounds of throughput capacity and average packet delay are derived in terms of the number of social spots, the size of the mobility region, and the decay factor of the power-law distribution. By identifying these key impact factors of performance mathematically, we find three possible regimes for the performance limits. Our results can be applied to predict the network performance of real-world scenarios and provide insight on the design and deployment of future vehicular networks.**

***Index Terms*—Capacity scaling laws, network delay, social-proximity, vehicular networks.**

I. Introduction

EMERGING vehicular ad hoc networks (VANETs) target to incorporate wireless communications and informatics technologies into the road transportation system, making isolated vehicles wirelessly connected. In the networks of connected vehicles, information generated by the vehicle-borne computer and control system, on-board sensors, or passengers can be effectively disseminated among vehicles in proximity by means of over-the-air communications, such as Dedicated Short-Range Communications (DSRC) [1]. Without the assistance of any built infrastructure, VANETs facilitate a variety of attractive applications to the passengers on board, relating to safety (e.g., collision detection, lane change warning, and cooperative merging) and infotainment (e.g., mobile office, points of interest, and other valuable information sharing) [2]–[5]. With rapidly evolving concepts of building applications, not only can VANETs make the transportation system safer and more efficient, but they can also revolutionize the in-vehicle experience of the passengers with media-rich infotainment.

There has been significant research interest in the field of mobile ad hoc networks in general and VANETs specifically, which has fascinated both the academia and the industry by its concepts and visions. Unlike the generic mobile ad hoc networks, VANETs present unique characteristics in terms of mobility, density, and applications, which accordingly impose distinguished challenges on networking. *First*, in VANETs, vehicles have *map-restricted* and *localized* mobility with specific social features. Notably, for most of the time, a vehicle only moves within a bounded region related to the social life of the driver. For example, a vehicle often moves within a small area daily close to the driver's home, the work place, or the city center. Such a mobility feature has also been reported in [6] based on the analysis of the real-world mobility trace of taxis in the city of Warsaw, Poland. It is observed that the mobility of taxis is typically around certain social spots. *Second*, VANETs show high *spatial variations* of vehicle density [2]. The analysis of the Warsaw trace data in [6] also reveals that the density of vehicles within the proximity area of social spots is much higher than on average and follows the empirical heavy-tailed distribution. *Third*, VANETs are mainly involved in the *proximity-related* applications, such as safety message dissemination and localized social content sharing, since it is neither practical nor necessary to maintain a long-lasting unicast communication flow among vehicles over a long distance. Although VANETs have received extensive attentions, the in-depth investigations on asymptotic performance limits (e.g., throughput capacity and delay) are very limited. Such asymptotic results are critical to predict network performance in face of the large-scale networks of connected vehicles [7]. Thus, it is desirable to know the fundamental capability of VANETs especially with the specific features aforementioned, which motivates our work.

In this paper, we investigate the throughput capacity and average packet delay of the social-proximity urban VANET. Specifically, we model the urban area as a scalable grid with equal-length road segments and a set of social spots. Considering the localized and social features of a vehicle's mobility, we apply a restricted mobility model to each vehicle surrounding a fixed social spot with the spatial stationary distribution of the vehicle following a power-law decay from the social spot to the border of the mobility region. Over this network model, we consider the social-proximity applications such that the data traffic is delivered through unicast flows; and for each unicast flow, its source and destination vehicles belong to the same social spot. With a variant of the two-hop relay scheme [8] applied, we derive the bounds of throughput capacity and average packet delay and show how the asymptotic results

Manuscript received April 14, 2012; revised January 14, 2013; accepted April 07, 2013; approved by IEEE/ACM TRANSACTIONS ON NETWORKING Editor M. Liu. This work was supported by NSERC and General Motors under a joint research grant.

N. Lu, T. H. Luan, M. Wang, and X. Shen are with the Department of Electrical and Computer Engineering, University of Waterloo, Waterloo, ON N2L 3G1, Canada (e-mail: n7lu@uwaterloo.ca; hluan@uwaterloo.ca; m59wang@uwaterloo.ca; sshen@uwaterloo.ca).

F. Bai is with the ECI Lab, General Motors Corporation, Warren, MI 48092 USA (e-mail: fan.bai@gm.com).

Color versions of one or more of the figures in this paper are available online at http://ieeexplore.ieee.org.

Digital Object Identifier 10.1109/TNET.2013.2260558

This article has been accepted for inclusion in a future issue of this journal. Content is final as presented, with the exception of pagination.

depend on the inherent mobility pattern of the network that is characterized by the number of social spots, size of the mobility region, and the decay factor of the spatial distribution.

The main contributions of this paper are threefold.

- Our work represents the first theoretical study on the social-proximity vehicular networks. As vehicular communications are intensively affected by the social behaviors of drivers, we argue that to accurately model the social features of vehicle mobility is crucial for the study of vehicular communications.
- We provide a generic modeling framework to unveil the asymptotic performance limits of the social-proximity vehicular networks. We obtain the bounds on per-vehicle throughput, average per-vehicle throughput, and average packet delay.
- The attained asymptotic property of capacity and delay can be used to predict network performance and provide guidance on design and analysis for different application scenarios of VANETs.

The remainder of this paper is organized as follows. Section II surveys the related works. In Section III, we introduce the system models. Section IV summarizes the main results of the paper. We analyze the asymptotic throughput capacity and average packet delay with the proposed two-hop relay scheme in Section V. Section VI concludes the paper.

II. Related Work

The throughput capacity of wireless networks was initially investigated by Gupta and Kumar in [9], where it has been shown that the per-node throughput decays at least as $1/\sqrt{N}$ in the presence of N nodes in the network. Since then, the study of capacity scaling in different networking scenarios has received extensive attentions from academia (e.g., [7], [10], and [11]). The effect of nodal mobility on capacity scaling was first reported by Grossglauser and Tse in [12]. By applying an independent and identically distributed (i.i.d.) mobility model to each node, they have shown that striking performance gains in throughput capacity are achievable, however, at the expense of enlarged delay. Inspired by this result, many research studies have been done to understand the relationship between delay and capacity of wireless networks under a variety of mobility models, such as i.i.d. mobility [8], [13], random walk [14], Brownian motion [15], and Lévy mobility [16]. However, these mobility models considered in aforementioned studies rely on the assumption that each node can visit the entire network equally likely following certain ergodic mobility processes.

By noticing that nodes often spend most of the time in proximity of a few preferred places within a localized area, some researchers have studied the throughput and delay under the restricted node mobility, which is more realistic to characterize mobility traces of humans, animals, and vehicles. Li *et al.* [17] investigated the impact of a restricted mobility model on throughput and delay of a cell-partitioned network. They found that smooth throughput–delay tradeoffs can be obtained by controlling the mobility pattern of nodes. Unlike the network in [17] showing the homogeneous node density, Garetto and Leonardi [18] considered heterogeneous node densities under restricted mobility model, in which each node moves around a fixed home-point according to a Markov process, and the stationary distribution of the node location decays as a power-law of exponent δ with the distance from the home-point. They showed that throughput–delay tradeoffs can be improved by restricting the node mobility and it is possible to achieve $\Theta(1/\log^2(N))$[1] throughput and $O(\log^4(N))$ delay by using a sophisticated bisection routing scheme. Instead of exploring the full range of possible delay–capacity tradeoffs, Ciullo *et al.* [19] studied the impact of correlated mobility on performance of delay and throughput. They considered a mobility model in which nodes in the network are grouped and each group, occupying a disc area, moves following i.i.d. mobility. The movements of different nodes belonging to the same group are restricted and correlated. It was shown that the correlated mobility pattern has significant impact on asymptotic network performance, and it is possible to achieve better delay and throughput performance than that shown in [13]. However, the capacity and delay are still unclear when we consider the proximity-related applications and the specific mobility features of vehicles.

For vehicular networks, the impact of road geometry and network topology on the capacity was investigated in [20]–[22]. In [23], Wang *et al.* considered a general multicast capacity scaling for an arterial road system. In [24], Wang *et al.* studied the throughput capacity of VANETs with infrastructure support. In [25], Zhang *et al.* analyzed multicast capacity of VANETs under delay constraint. All these works assume uniformly distributed vehicles in the network. This assumption may not be true for the urban area, where vehicle densities in different regions are highly diversified. Therefore, it is desirable to consider inhomogeneous vehicle densities in the network. Moreover, unlike these works except [25] that have not considered network delay, it is one of the key focuses of this paper to study the performance of average packet delay. It is noted that our previous work [26] has investigated this subject, however, only for a special case in which the number of social spots increases linearly with the population of vehicles and the size of mobility region is considered fixed.

III. System Model

A. Street Pattern

The geographic area where the network is deployed is modeled as a grid-like street layout, which consists of a set of M vertical roads intersected with a set of M horizontal roads, as shown in Fig. 1. Each line segment of equal length represents a road segment with bidirectional vehicle traffic. The grid street pattern is very common in many cities, such as Houston, TX, USA, and Portland, OR, USA [27]. In the model, M is used to characterize the scale of the city grid. For example, M is roughly 100 for the downtown area of Toronto, ON, Canada [28]. In addition, the city grid is considered as a torus of unit area to eliminate the border effects, which is a common

[1]We use standard order notations in the paper: Given nonnegative functions $f_1(n)$ and $f_2(n)$, $f_1(n) = O(f_2(n))$ means $f_1(n)$ is asymptotically upper-bounded by $f_2(n)$; $f_1(n) = \Omega(f_2(n))$ means $f_1(n)$ is asymptotically lower-bounded by $f_2(n)$; and $f_1(n) = \Theta(f_2(n))$ means $f_1(n)$ is asymptotically tight-bounded by $f_2(n)$; $f_1(n) = \omega(f_2(n))$ means $f_1(n)$ is asymptotically dominant with respect to $f_2(n)$; $f_1(n) = o(f_2(n))$ means $f_1(n)$ is asymptotically negligible with respect to $f_2(n)$.

This article has been accepted for inclusion in a future issue of this journal. Content is final as presented, with the exception of pagination.

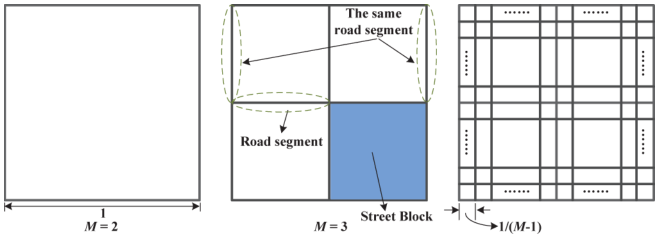

Fig. 1. Grid-like street layout.

TABLE I
USEFUL NOTATIONS

Symbol	Description
N	The number of vehicles in the network
M	The number of parallel roads in the grid
G	The number of road segments in the grid
C	The number of street blocks in the grid
ψ	Network density
V	The number of social spots
$\mathbf{S}$	The set of social spots, $\mathbf{S} = \{S_1, \ldots, S_V\}$
H_k	Vehicle k's social spot, $H_k \in \mathbf{S}$
ν	Exponent of V
κ	Exponent of $\mathcal{A}$
$\mathcal{A}$	The outermost tier of vehicle's mobility region
π'_α	The steady-state location probability of each vehicle on a segment of $Tier(\alpha)$
γ	The decay factor
r	The communication radius of the vehicle
Δ	The guard factor
$\mathbf{\Phi}$	The family of social-proximity vehicular networks
$\lambda(\Phi)$	Per-vehicle throughput
$\widetilde{\lambda}(\Phi)$	Average per-vehicle throughput
$\mathcal{D}(\Phi)$	Average packet delay
p_{ac}	The probability of a randomly selected road segment being active at a time slot
d_i^N	The vehicle density of road segment i
$\underline{d}_i^N$	The lower bound of d_i^N
$\overline{d}_i^N$	The upper bound of d_i^N
F_i	The rectangular area of $2\mathcal{A}(2\mathcal{A}-1)$ street blocks centered at road segment i
F_i^s	The number of social spots in F_i
S_j^v	The number of $\mathbb{S}$-$\mathbb{D}$ pairs associated with social spot S_j
$\mathcal{N}_i$	The number of vehicles on road segment i during a time slot
$\mathcal{N}_i^{\mathbb{SD}}$	The number of $\mathbb{S}$-$\mathbb{D}$ pairs on road segment i during a time slot
$P(\Phi)$	The average number of road segments where there are at least two vehicles during a time slot
$Q(\Phi)$	The average number of road segments where there is at least one $\mathbb{S}$-$\mathbb{D}$ pair during a time slot

practice to avoid tedious technicalities [18]. A summary of the mathematical notations used in the paper is given in Table I.

Let C denote the number of street blocks in the grid. The total number of road segments (the road section between any two neighboring intersections) is therefore $G = 2C = 2(M-1)^2$. We define the *network density* $\psi = \frac{N}{G} = \frac{N}{2(M-1)^2}$, where N is the total number of vehicles on the roads. Since N would tend to infinity in the asymptotic study, the city size, determined by M, cannot be fixed and should be scalable as well. Let $\Theta(1) \leq \psi \leq o(N)$ to avoid two extreme cases that are not practical in real-world scenarios: 1) when $\psi = o(1)$, the city size increases faster than the population of vehicles; and 2) when $\psi = \Theta(N)$, the city size is fixed such that the network density will become extremely high when more and more vehicles appear in the city. Note that ψ can represent the average vehicle density on each road segment. However, as each vehicle moves following the mobility model with social features, the spatial distribution of vehicles is inhomogeneous, as examples shown in Fig. 3(b) and (c). It can be seen that a network with a very large M and a relatively large ψ can represent metropolitan areas like New York City, NY, USA, whereas for a small town, M and ψ are relatively small. Therefore, from a macroscopic view, the grid street pattern with different values of M and ψ can model urban scenarios of different scales.

B. Socialized Mobility Model

Markovian Mobility Pattern: We consider the city grid, as shown in Fig. 1, where time is slotted with equal duration. The road segments are indexed from 1 to G, and vehicle nodes are indexed from 1 to N. Vehicles move independently from each other in the network. The mobility of a vehicle k follows a discrete-time Markovian process, denoted by $\mathcal{C}_k, k \in \{1, 2, \ldots, N\}$, which is uniquely represented by a one-dimensional G-state ergodic Markov chain. $\mathcal{C}_k(t) = i$ if vehicle k appears on road segment i, $i \in \{1, 2, \ldots, G\}$, at time-slot t, $t \in \{1, 2, \ldots, T\}$. Let P_k^{ij} denote the transition probability that vehicle k moves from road segment i to the next road segment j, $j \in \{1, 2, \ldots, G\}$. Let $\mathbf{P}_k = \{P_k^{ij}\}_{G\times G}$ denote the transition probability matrix of $\mathcal{C}_k$; the element P_k^{ij} in $\mathbf{P}_k$ is nonzero only if j is a neighboring road segment of i. The steady-state location distribution of vehicle k is $bm\pi_k = \{\pi_k(i)\}_{1\times G}$, where $\pi_k(i)$ denotes the long-term proportion of time that vehicle k stays on road segment i. In [29], it has been shown that the capacity region only depends on how the node location distributes in the steady state. In [30], it has been shown that the Markovian mobility model converges to its steady-state location distribution at an exponential rate. Therefore, we will focus on the steady-state location distribution of the vehicles.

Restricted Mobility Region With Social Spot: The mobility region of each vehicle is restricted and associated with a fixed social spot. The social spot is geographically the center of a certain street block, as shown in Fig. 2. Let V denote the number of social spots in the grid. We assume that all the social spots in the grid are uniformly distributed and, therefore, do not consider the inhomogeneous distribution of social spots in this study. Indexing all the street blocks from 1 to C, we denote by $\mathbf{S} = \{S_1, S_2, \ldots, S_V\} \subseteq \{1, 2, \ldots, C\}$ the set of social spots. Since we are only interested in the order of performance limits, let $V = |\mathbf{S}| = \lceil C^\nu \rceil$, where $\nu \in (0, 1]$. It can be seen that $V = \Theta((N/\psi)^\nu)$, represented by a power function of N. When $\nu = 1$, all the street blocks in the network will be social spots. In addition, we consider all the intermediate cases of ν between 0 and 1 in the paper.[2] Each vehicle uniformly and independently selects one social spot out of all the social spots. Let $\mathbf{H}_N = (H_1, H_2, \ldots, H_N)$ denote the vector that collects the locations of all the vehicles' social spots, with each element $H_k \in \mathbf{S}$, denoting the index of the street block where vehicle k's

[2]We do not consider the extreme case in which $\nu = 0$. When $\nu = 0$, there is only one social spot in the network.

This article has been accepted for inclusion in a future issue of this journal. Content is final as presented, with the exception of pagination.

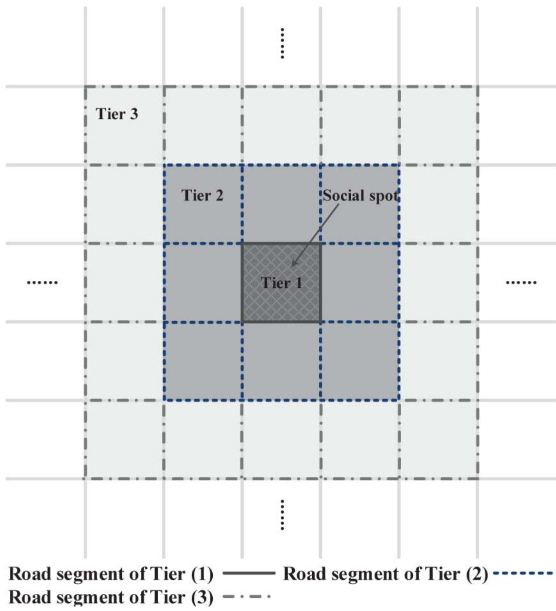

Fig. 2. Restricted and socialized mobility with different tiers centered at a social spot for a given vehicle.

social spot is located. The set $\mathbf{S}$ is fixed once the network is defined.

The mobility region of each vehicle is composed of multiple tiers co-centered at its social spot, as shown in Fig. 2. $\mathrm{Tier}(1)$ of the mobility region is collocated with the social spot and contains four road segments. The adjacent street blocks surrounding $\mathrm{Tier}(1)$ form $\mathrm{Tier}(2)$, and so forth. Let $\mathrm{Tier}(\mathcal{A})$ denote the outermost tier of the mobility region, where $\mathcal{A} = \Theta(M^{\kappa}) = \Theta((N/\psi)^{\frac{\kappa}{2}}) \leq \lfloor \frac{M}{2} \rfloor$, $\kappa \in [0, 1)$. When $\kappa = 0$, the size of the mobility region is fixed and does not scale with the city grid. It can be easily derived that $\mathrm{Tier}(\alpha)$, $\alpha \in \{1, 2, \ldots, \mathcal{A}\}$, contains $16\alpha - 12$ road segments. Therefore, the mobility of each vehicle is constrained in $\mathcal{A}$ tiers with a total number of $\sum_{\alpha=1}^{\mathcal{A}} 16\alpha - 12 = 4\mathcal{A}(2\mathcal{A} - 1)$ road segments, and further the mobility region covers an area of $(\mathcal{A} + 1)^2/C = \Theta((N/\psi)^{\kappa-1})$. For a randomly selected $\mathrm{Tier}(\alpha)$, a vehicle has equal steady-state probability to appear on each road segment. Let π'_{α} denote the steady-state location probability of each vehicle on one of the road segments of $\mathrm{Tier}(\alpha)$. From $\mathrm{Tier}(1)$ to $\mathrm{Tier}(\mathcal{A})$, the steady-state location probability of vehicles is modeled to exponentially decay as a power-law function with exponent $\gamma > 0$. Therefore, we have $\pi'_{\alpha} = \alpha^{-\gamma}\pi'_1$, which indicates that a vehicle is more likely to stay in the area near its social spot. The same model has been used in [18], and its accuracy is validated in [6] through real-world measurements. As the summation of steady-state probability on road segments equals to 1, i.e.,

$$\sum_{\alpha=1}^{\mathcal{A}} (16\alpha - 12)\pi'_{\alpha} = \sum_{\alpha=1}^{\mathcal{A}} (16\alpha - 12)\alpha^{-\gamma}\pi'_1 = 1$$

we have

$$\pi'_1 = \frac{1}{\sum\limits_{\alpha=1}^{\mathcal{A}} (16\alpha - 12)\alpha^{-\gamma}}. \tag{1}$$

Lemma 1: Given that $\kappa > 0$, as $N \to \infty$, $\pi'_1 = \Theta((N/\psi)^{-\kappa(1-\frac{1}{2}\gamma)})$, for $0 < \gamma < 2$; $\pi'_1 = \Theta(\frac{1}{\log(N/\psi)})$, for $\gamma = 2$; π'_1 converges to a constant value, for any $\gamma > 2$.

This lemma can be proved by applying results of partial sums of p-series [31] directly. Note that when $\kappa = 0$, π'_1 is constant for all γ. Using the mobility model discussed above, the network presents inhomogeneous vehicle densities. Fig. 3 shows the example of vehicle density in the network when the vehicles are uniformly distributed and follow the socialized mobility model, respectively.

C. Traffic Model

We consider that there exist N unicast flows concurrently in the network. Each vehicle is exactly the source of one unicast flow and the destination of another unicast flow. We consider the case in which the source and destination vehicles of each unicast flow have the same social spot. This is motivated by the dominant proximity applications in vehicular communications. As such, the source and destination vehicles of each unicast flow are spatially close to each other. Without loss of generality, N is considered to be even. We sort the index of vehicles such that vehicle k communicates with vehicle $k+1$, $k \in \{1, 3, 5, \ldots, N-1\}$, and each communication pair independently and uniformly chooses a social spot from $\mathbf{S}$. The packet arrives in each unicast flow at an average rate η.

D. Communication Model

Since the communication range of a vehicle is geographically limited in practice, the communication radius should scale with M. Let $r = \frac{1}{M-1}$ denote the communication radius of each vehicle that can always cover the entire road segment, as shown in Fig. 7. Without loss of generality, a pair of vehicles can communicate only when they are on the same road segment at the same time-slot, and the transmission spans the whole time-slot. Although the communication model has been simplified, such simplification does not affect the order of the bounds of throughput capacity and average packet delay derived in the paper. The success or failure of a transmission is determined by the protocol model defined in [9] as follows. The transmission from vehicle i to vehicle j can be successful during time-slot t if and only if the following condition holds: $d_{kj}(t) \geq (1+\Delta)r$, for every other vehicle k transmitting simultaneously, where $d_{kj}(t)$ denotes the Euclidean distance between vehicle k and j at time-slot t, and $\Delta > 0$ is a guard factor.

E. Definitions of Throughput and Delay

We denote by $\mathbf{\Phi}(N, \psi, \gamma, \mathcal{A}(\kappa), \mathbf{S}(\nu), \mathbf{H}_N)$ the family of social-proximity vehicular networks that we consider in the paper. Let $L_k(T)$ be the number of packets received by the destination of flow k, $k \in \{1, 2, \ldots, N\}$, up to time T; let $\mathcal{D}_k(T)$ be the integrated delay of packets received by the destination of flow k up to time T. An asymptotic per-vehicle throughput $\lambda(\Phi)$ and average delay $\mathcal{D}(\Phi)$ of $\mathbf{\Phi}$ are said feasible if there exist a scheduling policy and an N_0 such that for any $N > N_0$, we have

$$\lim_{T \to \infty} \mathbf{Pr}\left(\frac{L_k(T)}{T} \geq \lambda(\Phi), \forall k\right) = 1 \tag{2}$$

$$\lim_{T \to \infty} \mathbf{Pr}\left(\frac{\mathcal{D}_k(T)}{L_k(T)} \leq \mathcal{D}(\Phi), \forall k\right) = 1. \tag{3}$$

This article has been accepted for inclusion in a future issue of this journal. Content is final as presented, with the exception of pagination.

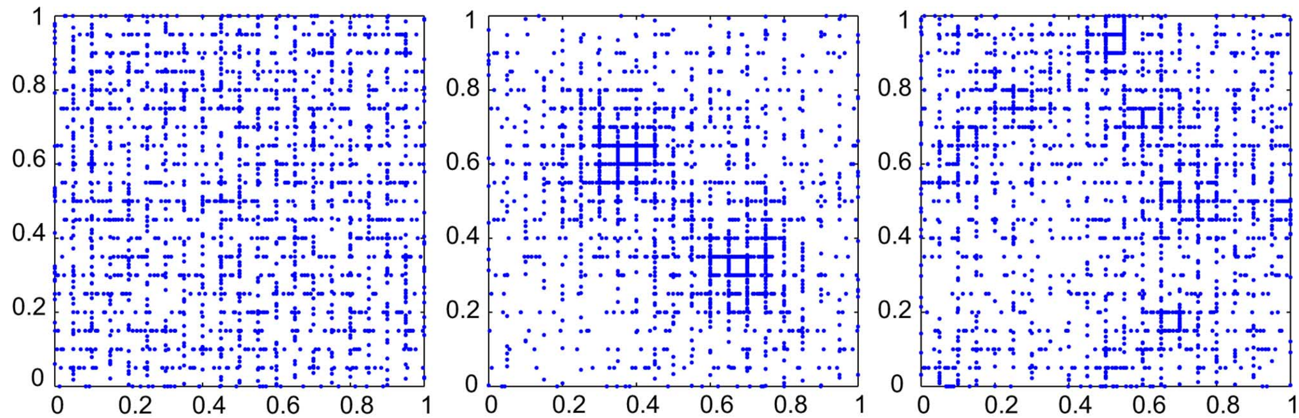

(a) (b) (c)

Fig. 3. Examples of (a) homogeneous and (b), (c) inhomogeneous distributions of vehicles in the network, in the case of $N = 2000$, $M = 21$, $\mathcal{A} = 10$, and $\gamma = 2$. (a) Uniform distribution. (b) Distribution with social spots ($V = 2$). (c) Distribution with social spots ($V = 10$).

Specifically, an average per-vehicle throughput $\widetilde{\lambda}(\Phi)$ of $\mathbf{\Phi}$ is said feasible if there exist a scheduling policy and an N_0, such that for any $N > N_0$, the following holds:

$$\lim_{T\longrightarrow\infty} \mathbf{Pr}\left(\frac{\sum_{k=1}^{N} L_k(T)}{NT} \geq \widetilde{\lambda}(\Phi)\right) = 1. \tag{4}$$

IV. Summary of Main Results

This section presents the summary of our main results. The formal statement of the results (Theorems 1–3) and the derivations are given in Section V.

The results of capacity and delay obtained in the analysis demonstrate three possible regimes depending on different values of κ and ν, as shown in Fig. 4. Recall that the size of mobility region and the number of social spots scale as $\Theta((N/\psi)^{\kappa-1})$ and $\Theta((N/\psi)^{\nu})$, respectively.

1) *Dense regime:* When $\kappa + \nu > 1$, the sum of all mobility regions associated with different social spots is $\Theta((N/\psi)^{\kappa+\nu-1}) = \omega(1)$, which indicates that V different mobility regions are overlapped and fully cover the city grid.
2) *Sparse regime:* When $\kappa + \nu < 1$, the sum of all different mobility regions is $o(1)$, which results in V typically isolated mobility regions sparsely distributed in the city grid.
3) *Balanced regime:* When $\kappa + \nu = 1$, the sum of all different mobility regions has the same scale with the grid area, making the mobility area of vehicles perfectly fit the grid area in the order sense.

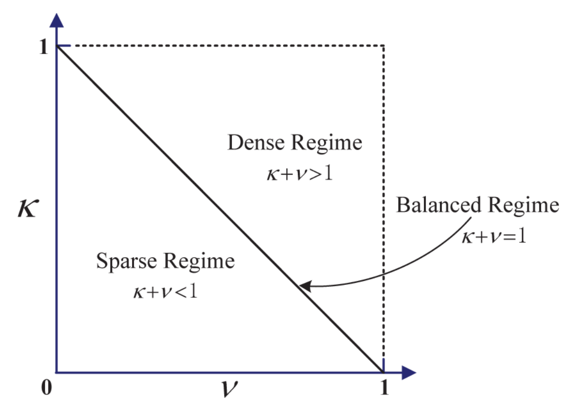

Fig. 4. Regimes for asymptotic performance limits with respect to κ and ν.

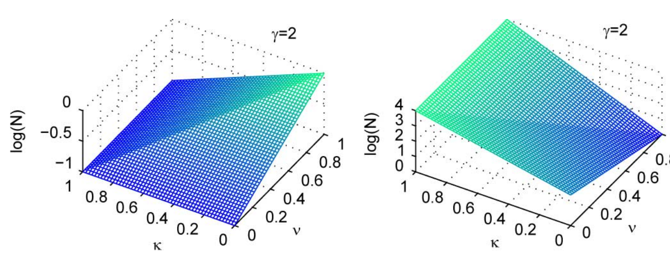

(a) (b)

Fig. 5. Per-vehicle throughput and average packet delay. (a) Lower bound of per-vehicle throughput. (b) Upper bound of average packet delay.

A graphical representation of our results is reported in Figs. 5 and 6. The results are shown in log-scale in terms of κ and ν, with $\psi = \Theta(1)$. For example, "-0.5" corresponds to a throughput of $\Theta(\frac{1}{\sqrt{N}})$. Fig. 5(a) shows the lower bound of the per-vehicle throughput capacity for $\gamma = 2$. In the dense regime, bounds of per-vehicle throughput capacity are dominated by κ given γ and ψ. It is observed that a large κ indicates a large size of mobility region, which results in decrease in per-vehicle throughput because: 1) the contact probability of a pair of vehicles is reduced; and 2) different mobility regions are largely overlapped so that potentially increase the vehicle density. In the sparse regime, the performance is mainly dominated by ν. When ν tends to 1, the number of vehicles associated with each social spot is significantly reduced, avoiding a high vehicle density in the proximity of social spots. Therefore, the throughput performance is enhanced with a large ν. The performance decreases in the sparse regime when $\kappa + \nu$ tends to zero due to increasing empty area in the city grid where there is no any packet transmission occurs. When $\kappa + \nu = 1$, the network achieves optimal bounds of per-vehicle throughput capacity since the geographic area of the city grid, i.e., the spatial resource of the network, is just fully utilized for packet transmissions. From Fig. 5(b), the same insight on average packet delay can be obtained. Therefore, it is possible to achieve almost constant (except for the polylogarithmic factor)

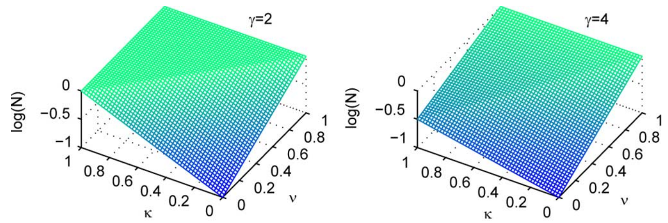

(a) (b)

Fig. 6. Average per-vehicle throughput. (a) Lower bound for $\gamma = 2$. (b) Lower bound for $\gamma = 4$.

per-vehicle throughput and average packet delay, i.e., in the case of $\kappa = 0$ and $\nu = 1$.

The average per-vehicle throughput represents a global performance metric of the network with inhomogeneous vehicle densities. Fig. 6(a) and 6(b) demonstrates the average per-vehicle throughput for $\gamma = 2$ and $\gamma = 4$, respectively. For $\gamma = 2$, almost constant average per-vehicle throughput is achievable with high probability in the dense regime. However, in this case, the per-vehicle throughput may degrade dramatically, as shown in Fig. 5(a), in some hot area that is covered by a large number of different overlapped mobility regions. With a larger value of γ, e.g., $\gamma = 4$, the vehicles usually move in a very limited area centered at the social spot. Due to the limited spatial resource, the total number of concurrent transmissions is reduced. Therefore, the average per-vehicle throughput decreases since the geographic area of the city grid is not fully used for packet transmissions.

It has been shown that the performance metrics of interest depend on inherent mobility patterns of the network. Notice that the parameters of the socialized mobility are not easy to obtain, although they can be extracted from real-world mobility traces of vehicles. Once the mobility pattern of the real-world scenario is determined, our results can be applied to predict network performance, at least in the order sense. We provide an example in the following. Consider a network of 10^4 vehicles with parameters of mobility model $\kappa = 0.5$, $\nu = 0.7$, and $\gamma = 2$. The bandwidth of point-to-point link is 1 Mb/s. From the results obtained in the analysis, neglecting polylogarithmic factors and constant factor ψ, a per-vehicle throughput of around 10 kb/s is achievable. If we consider a duration of 1 ms for each time-slot, the time to deliver a packet could be from seconds to days. We notice that the delay performance may not satisfy requirements of many applications. It is important to note that there exists a throughput–delay tradeoff for a given mobility pattern. The throughput and delay achieved in the example is under the proposed two-hop relay scheme that is elaborated in Section V. Better delay performance can be obtained by using other forwarding schemes, such as multihop scheme with or without packet redundancies, however with a lower throughput. Considering another mobility pattern where $\kappa = 0.2$ and $\nu = 0.8$, the per-vehicle throughput is around 150 kb/s, and the average packet delay could be at most several seconds. It can be seen that when κ and ν tend to 0 and 1, respectively, the delay is small enough for many applications by using the two-hop relay scheme, indicating that it is not necessary to sacrifice throughput to improve the network delay. Therefore, another implication

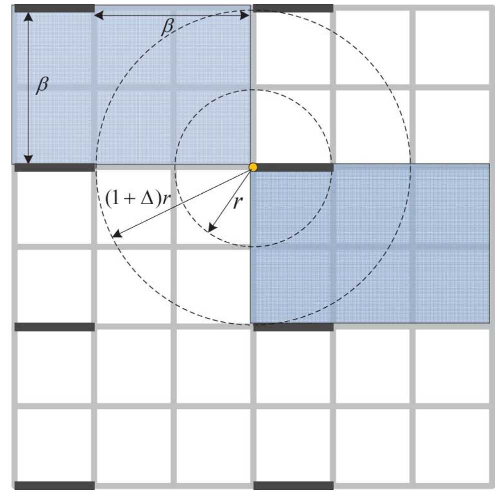

Fig. 7. Example of noninterfering transmission group of road segments.

from our results is that it is beneficial to design suitable forwarding schemes according to different mobility patterns of the network.

V. Asymptotic Capacity and Delay Analysis

In this section, we first propose a two-hop relay scheme to deliver the packets from the source to the destination. After that, we derive the bounds of per-vehicle throughput capacity, average per-vehicle throughput, and average packet delay of the network, which are stated in Theorems 1–3, respectively.

A. Two-Hop Relay Scheme

Let packets be transmitted by using a two-hop relay scheme $\mathcal{X}$: A packet is either transmitted directly from the source to the destination, or relayed through one intermediate vehicle from the source to the destination. The packet transmission consists of two phases:

$\mathcal{X}$ -I: Each road segment in the network becomes "active" in every $1/p_{\rm ac}$ time-slots.[3]

$\mathcal{X}$-II: For each active road segment where there are at least two vehicles:

1) If there exists at least one source–destination ($\mathbb{S}$-$\mathbb{D}$) pair on the road segment, one pair is uniformly selected. If the source has a buffering packet for transmission to the destination, it transmits the packet and evicts it from the buffer after the transmission; otherwise, the source stays idle.
2) If there is not any $\mathbb{S}$-$\mathbb{D}$ pair on the road segment, a vehicle, e.g., v_A, is uniformly selected out of all vehicles on this road segment to be the source or the destination equally likely, and in the meantime another vehicle, e.g., v_B, is independently and uniformly selected over the rest of vehicles to be the relay.
   - If v_A is the source, a source-to-relay transmission from v_A to v_B is scheduled. If v_A has a buffering packet to transmit, v_A transmits the packet to v_B and evicts the packet from the buffer; otherwise, v_A remains idle.

[3]A road segment is active when vehicles on the road segment can transmit successfully without any interference of transmissions from other road segments. The value of $p_{\rm ac}$ is discussed later in the section.

- If v_A is the destination, a relay-to-destination transmission from v_B to v_A is scheduled. If v_B has a buffering packet destined for v_A, v_B transmits the packet to v_A and evicts the packet from the buffer; otherwise, v_B remains idle.

Next, we calculate the value of $p_{\rm ac}$, which is the probability of a randomly selected road segment being active at a time-slot. As shown in Fig. 7, we partition the network into equal-size subareas. Each subarea consists of $\beta(\beta+1)$ street blocks, where β is an integer number. The road segments highlighted in each subarea in Fig. 7 constitute one noninterfering transmission group, such that simultaneous transmissions within one noninterfering group do not interfere with each other. Totally, there are $2\beta(\beta+1)$ road segments within one subarea, and collectively $2\beta(\beta+1)$ noninterfering groups in the network. With noninterfering groups transmitting iteratively, each noninterfering group becomes active every $1/p_{\rm ac} = 2\beta(\beta+1)$ time-slots. This indicates that the vehicles on one specific road segment obtain a transmission opportunity with probability $p_{\rm ac}$ at a randomly selected time-slot. With the grid scale of M, the minimum distance between any two neighboring road segments of a noninterfering group is $\frac{\beta}{M-1}$. With the protocol model applied, we have

$$\beta/(M-1) \geq (1+\Delta)r.$$

With $r = 1/(M-1)$, we have $\beta \geq 1+\Delta$. We set $\beta = \lceil 1+\Delta \rceil$. By substituting it into $1/[2\beta(\beta+1)]$, we have

$$p_{\rm ac} = 1/(2\lceil 1+\Delta\rceil \lceil 2+\Delta\rceil).$$

B. Bounds of Per-Vehicle Throughput Capacity

Next, we derive the bounds of the per-vehicle throughput capacity with the two-hop relay scheme $\mathcal{X}$, which are formally stated in Theorem 1. We first try to obtain an important result of vehicle density of a generic road segment (Lemma 3) by applying Chernoff bounds (Lemma 2) and the Vapnik–Chervonenkis Theorem, which gives the uniform convergence in the weak law of large numbers.

To characterize the vehicle spatial inhomogeneities of the network, inspired by [32], we define the vehicle density $(\text{vehicles}/\text{road segment})$ of a generic road segment i by

$$d_i^N = \sum_{k=1}^{N} E[\mathbb{I}_{\mathcal{C}_k(t)=i} | \mathbf{H}_N] \tag{5}$$

where $\mathbb{I}_{\mathcal{C}_k(t)=i}$ is the indicator variable that takes value 1 if $\mathcal{C}_k(t) = i$, and 0 otherwise.

Lemma 2 (Chernoff bounds [33]): Let X be a sum of n independent random variables $\{X_i\}$, with $X_i \in \{0,1\}$ for all $i \leq n$. Write $\mu' = E[X] = E[X_1] + \ldots + E[X_n]$. Then, for any $0 < \varepsilon \leq 1$

$$\mathbf{Pr}(X > (1+\varepsilon)\mu') \leq e^{-\frac{\varepsilon^2}{2+\varepsilon}\mu'}$$
$$\mathbf{Pr}(X < (1-\varepsilon)\mu') \leq e^{-\frac{\varepsilon^2}{2}\mu'}.$$

Lemma 2 is a well-known result and will be used to prove the following important lemma that presents a bound of d_i^N.

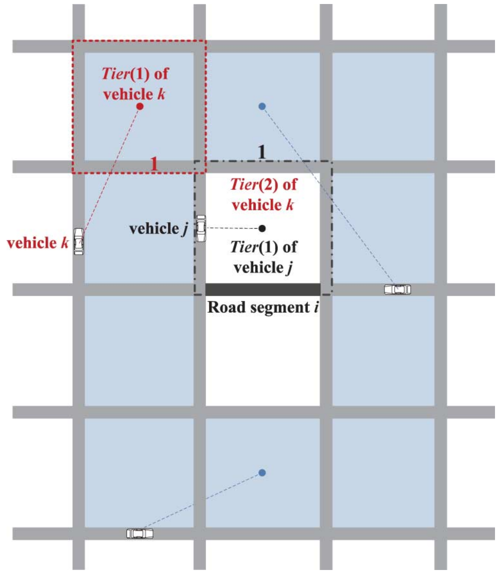

Fig. 8. Example of one given road segment contained by different vehicles' mobility regions.

Lemma 3: The following bounds of the vehicle density d_i^N hold *w.h.p.*,[4] $\forall i \in \{1, 2, \ldots, G\}$.

i) When $\kappa + \nu > 1$

$$d_i^N = \begin{cases} \Omega(\psi), O(\psi(N/\psi)^{\frac{1}{2}\kappa\gamma}), & 0 < \gamma < 2 \\ \Omega(\frac{\psi}{\log(N/\psi)}), O(\frac{\psi(N/\psi)^{\kappa}}{\log(N/\psi)}), & \gamma = 2 \\ \Omega(\frac{\psi}{(N/\psi)^{\kappa(\frac{1}{2}\gamma-1)}}), O(\psi(N/\psi)^{\kappa}), & \gamma > 2. \end{cases}$$

ii) When $\kappa + \nu \leq 1$

a) $\kappa = 0$, $d_i^N = O(\psi(N/\psi)^{1-\nu}\log(N/\psi))$;

b) $\kappa \neq 0$,

$$d_i^N = \begin{cases} O\left(\frac{\psi \log(N/\psi)}{(N/\psi)^{\nu+\kappa(1-\frac{1}{2}\gamma)-1}}\right), & 0 < \gamma < 2 \\ O(\psi(N/\psi)^{1-\nu}), & \gamma = 2 \\ O(\psi(N/\psi)^{1-\nu}\log(N/\psi)), & \gamma > 2. \end{cases}$$

Proof: The proof of Lemma 3 consists of three parts in terms of different values of ν and κ.

(i) $0 < \nu < 1$ and $\kappa + \nu > 1$:

First, we show that Lemma 3 holds for $0 < \nu < 1$ and $\kappa + \nu > 1$. We denote by F_i the rectangular area of $2\mathcal{A}(2\mathcal{A}-1)$ street blocks centered at road segment i, as shown in Fig. 8. If the social spot of vehicle k is not located in F_i, $E[\mathbb{I}_{\mathcal{C}_k(t)=i}] = 0$. In other words, vehicles whose social spots are located in F_i contribute d_i^N. Let $F_i^{\rm s}$ denote the number of social spots contained in F_i. Intuitively, a social spot describes a mobility region of vehicles that are associated with this social spot. The vehicle density of a road segment depends on how many mobility regions contain this road segment. Therefore, the number of social spots in an area plays an important role in determining the vehicle density of a road segment, and further the throughput capacity. We first bound $F_i^{\rm s}$, for all $i \in \{1, 2, \ldots, G\}$. By definition, we have

$$F_i^{\rm s} = \sum_{j=1}^{V} \mathbb{I}_{Sj \in Fi} \tag{6}$$

[4] As $N \longrightarrow \infty$, the probability of the event approaches 1.

This article has been accepted for inclusion in a future issue of this journal. Content is final as presented, with the exception of pagination.

where $\mathbb{I}_{S_j \in F_i}, \forall j \in \{1, 2, \ldots, V\}$, are i.i.d. Bernoulli random variables with expectation $\mu = \frac{2\mathcal{A}(2\mathcal{A}-1)}{C}$. Inspired by [32], from Lemma 2, we have

$$\mathbf{Pr}\left\{F_i^{\mathrm{s}} < \frac{1}{2}E[F_i^{\mathrm{s}}] = \frac{1}{2}V\mu\right\} < e^{-\frac{1}{8}V\mu}$$
$$\mathbf{Pr}\left\{F_i^{\mathrm{s}} > 2E[F_i^{\mathrm{s}}] = 2V\mu\right\} < e^{-\frac{1}{3}V\mu} < e^{-\frac{1}{8}V\mu}.$$

It can be obtained that $\mu = \Theta((N/\psi)^{\kappa-1})$. By applying the union bound, we have

$$\begin{aligned}\mathbf{Pr}&\left\{\bigcap_i \left\{\frac{1}{2}E[F_i^{\mathrm{s}}] < F_i^{\mathrm{s}} < 2E[F_i^{\mathrm{s}}]\right\}\right\}\\ &= 1 - \mathbf{Pr}\left\{\bigcup_i \left\{F_i^{\mathrm{s}} < \frac{1}{2}E[F_i^{\mathrm{s}}] \cup F_i^{\mathrm{s}} > 2E[F_i^{\mathrm{s}}]\right\}\right\}\\ &\geq 1 - \sum_{i=1}^{G} \mathbf{Pr}\left\{F_i^{\mathrm{s}} < \frac{1}{2}E[F_i^{\mathrm{s}}] \cup F_i^{\mathrm{s}} > 2E[F_i^{\mathrm{s}}]\right\}\\ &\geq 1 - G2e^{-\frac{1}{8}V\mu}.\end{aligned}$$

For $\kappa + \nu > 1$, $G2e^{-\frac{1}{8}V\mu} \to 0$, as $N \to \infty$. Therefore, *w.h.p.*, we get

$$\frac{1}{2}E[F_i^{\mathrm{s}}] < F_i^{\mathrm{s}} < 2E[F_i^{\mathrm{s}}] \qquad \forall i \in \{1, 2, \ldots, G\}. \tag{7}$$

Let $S_j^v = \sum_{k=1}^{N-1} \mathbb{I}_{H_k = S_j}$ denote the number of $\mathbb{S}$-$\mathbb{D}$ pairs associated with social spot S_j, where $\mathbb{I}_{H_k = S_j}$, $\forall k \in \{1, 3, \ldots, N-1\}$, are i.i.d. Bernoulli random variables with expectation $1/V$. From Lemma 2, for $0 < \varepsilon \leq 1$, we have

$$\mathbf{Pr}\left\{\frac{(1-\varepsilon)N}{2V} < S_j^v < \frac{(1+\varepsilon)N}{2V}\right\} \geq 1 - 2e^{-\frac{\varepsilon^2 N}{2(2+\varepsilon)V}}.$$

By applying union bound

$$\begin{aligned}\mathbf{Pr}&\left\{\bigcap_j \left\{\frac{(1-\varepsilon)N}{2V} < S_j^v < \frac{(1+\varepsilon)N}{2V}\right\}\right\}\\ &= 1 - \mathbf{Pr}\left\{\bigcup_j \left\{S_j^v < \frac{(1-\varepsilon)N}{2V} \cup S_j^v > \frac{(1+\varepsilon)N}{2V}\right\}\right\}\\ &\geq 1 - \sum_{j=1}^{V} \mathbf{Pr}\left\{S_j^v < \frac{(1-\varepsilon)N}{2V} \cup S_j^v > \frac{(1+\varepsilon)N}{2V}\right\}\\ &\geq 1 - V2e^{-\frac{\varepsilon^2 N}{2(2+\varepsilon)V}}.\end{aligned}$$

Since $V = \Theta((N/\psi)^{\nu})$ and $\nu \neq 1$, $V2e^{-\frac{\varepsilon^2 N}{(2+\varepsilon)V}} \to 0$, as $N \to \infty$. Therefore, *w.h.p.*, we get

$$\frac{(1-\varepsilon)N}{2V} < S_j^v < \frac{(1+\varepsilon)N}{2V} \qquad \forall j \in \{1, 2, \ldots, V\}. \tag{8}$$

By definition (5) and from (7) and (8), *w.h.p.*, we obtain, $\forall i$

$$\begin{aligned}\frac{1}{2}V\mu \cdot \frac{(1-\varepsilon)N}{V} \cdot \mathcal{A}^{-\gamma}\pi_1' = \underline{d}_i^N < d_i^N < \overline{d}_i^N\\ = 2V\mu \cdot \frac{(1+\varepsilon)N}{V} \cdot \pi_1'\end{aligned}$$

denoting by $\underline{d}_i^N$ and $\overline{d}_i^N$ the lower bound and upper bound of d_i^N, respectively. Letting $\varepsilon \to \infty$, we have $\underline{d}_i^N = \Theta\left(\pi_1'\psi(N/\psi)^{\kappa(1-\frac{1}{2}\gamma)}\right)$ and $\overline{d}_i^N = \Theta(\pi_1'\psi(N/\psi)^{\kappa})$. The assert follows according to Lemma 1 for (i).

(ii) $\nu = 1$:

To prove Lemma 3 for the case in which $\nu = 1$, we recall the Vapnik–Chervonenkis Theorem [34]. Some relevant definitions are first provided. A Range Space is a pair $(X, \mathcal{F})$, where X is a set and $\mathcal{F}$ is a family of subsets of X. For any $A \subseteq X$, we define $P_{\mathcal{F}}(A)$, the projection of $\mathcal{F}$ on A, as $\{F \cap A : F \in \mathcal{F}\}$. We say that A is *shattered* by $\mathcal{F}$ if $P_{\mathcal{F}}(A) = 2^A$, i.e., if the projection of $\mathcal{F}$ on A includes all possible subsets of A. The VC-dimension of $\mathcal{F}$, denoted by VC-d($\mathcal{F}$) is the cardinality of the largest set A that $\mathcal{F}$ shatters. If arbitrarily large finite sets are shattered, the VC dimension of $\mathcal{F}$ is infinite.

Vapnik–Chervonenkis Theorem: If $\mathcal{F}$ is a set of finite VC-dimension and $\{Y_j\}$ is a sequence of N i.i.d. random variables with common probability distribution P, then for every $\epsilon, \delta > 0$

$$\mathbf{Pr}\left\{\sup_{F \in \mathcal{F}}\left|\frac{1}{N}\sum_{j=1}^{N} \mathbb{I}_{Y_j \in F} - P(F)\right| \leq \epsilon\right\} > 1 - \delta \tag{9}$$

if

$$N > \max\left\{\frac{8\mathrm{VC}-\mathrm{d}(\mathcal{F})}{\epsilon}\log\frac{16e}{\epsilon}, \frac{4}{\epsilon}\log\frac{2}{\delta}\right\}. \tag{10}$$

We use the Vapnik–Chervonenkis Theorem to show that Lemma 3 holds for $\nu = 1$. Recall that F_i denotes the rectangular area of $2\mathcal{A}(2\mathcal{A}-1)$ street blocks centered at road segment i. $\sum_{k=1}^{N-1} \mathbb{I}_{H_k \in F_i}$, $k \in \{1, 3, \ldots, N-1\}$, is the number of $\mathbb{S}$-$\mathbb{D}$ pairs whose social spot falls into the region F_i. $\mathbf{Pr}(\mathbb{I}_{H_k \in F_i} = 1) = \frac{2\mathcal{A}(2\mathcal{A}-1)}{C} = \Theta((N/\psi)^{\kappa-1})$, $\forall k$. Let $\mathcal{F}$ be the class of all such F_i rectangular areas. It is easy to show that the VC-dimension of $\mathcal{F}$ is at most 4 [35]. Therefore, $\forall F_i$

$$\mathbf{Pr}\left\{\sup_{F_i \in \mathcal{F}}\left|\frac{\sum_{k=1}^{N-1} \mathbb{I}_{H_k \in F_i}}{N/2} - \frac{2\mathcal{A}(2\mathcal{A}-1)}{C}\right| \leq \epsilon\right\} > 1 - \delta.$$

The condition (10) holds when $\epsilon = \delta = \frac{\Delta_\epsilon \log(N/\psi)}{N/\psi}$, where $\Delta_\epsilon := \max\{8\mathrm{VC}-\mathrm{d}(\mathcal{F}), 16e\}$. Thus, the Vapnik–Chervonenkis Theorem states that

$$\begin{aligned}\mathbf{Pr}&\left\{\sup_{F_i \in \mathcal{F}}\left|\sum_{k=1}^{N-1} \mathbb{I}_{H_k \in F_i} - \Theta\left(\psi\left(\frac{N}{\psi}\right)^{\kappa}\right)\right| \leq \Theta\left(\psi\log\frac{N}{\psi}\right)\right\}\\ &> 1 - \frac{\Delta_\epsilon \log(N/\psi)}{N/\psi}.\end{aligned}$$

We conclude that *w.h.p.*, for $\kappa = 0$

$$\overline{d}_i^N = 2\max\left\{\sum_{k=1}^{N-1} \mathbb{I}_{H_k \in F_i}\right\}\pi_1' = \Theta(\psi\log(N/\psi)) \qquad \forall i$$

for $0 < \kappa < 1$, $\underline{d}_i^N = \Theta\left(\pi_1'\psi(N/\psi)^{\kappa(1-\frac{1}{2}\gamma)}\right)$ and $\overline{d}_i^N = \Theta(\pi_1'\psi(N/\psi)^{\kappa})$, $\forall i$. The assert follows according to Lemma 1 for $\nu = 1$.

(iii) $0 < \nu < 1$ and $\kappa + \nu \leq 1$:

We apply the Vapnik–Chervonenkis Theorem again to show this part. From (6), we have

$$\mathbf{Pr}\left\{\sup_{F_i \in \mathcal{F}} \left| \frac{\sum_{j=1}^{V} \mathbb{I}_{S_j \in F_i}}{V} - \frac{2\mathcal{A}(2\mathcal{A}-1)}{C} \right| \leq \epsilon \right\} > 1 - \delta.$$

The condition (10) holds when $\epsilon = \delta = \frac{\Delta_\epsilon \log(V)}{V} = \frac{\Delta_\epsilon \log(N/\psi)}{(N/\psi)^\nu}$. Thus

$$\mathbf{Pr}\left\{\sup_{F_i \in \mathcal{F}} \left| \sum_{j=1}^{V} \mathbb{I}_{S_j \in F_i} - \Theta\left(\left(\frac{N}{\psi}\right)^{\kappa+\nu-1}\right) \right| \leq \Delta_\epsilon \log\left(\frac{N}{\psi}\right) \right\}$$
$$> 1 - \frac{\Delta_\epsilon \log(N/\psi)}{(N/\psi)^\nu}. \tag{11}$$

Since $\kappa + \nu \leq 1$, we conclude that *w.h.p.*, $F_i^{\mathrm{s}} = O(\log(N/\psi))$, $\forall i$. From (8) and (11), the upper bound of vehicle density $\overline{d}_i^N = \Theta(\pi_1' \psi (N/\psi)^{1-\nu} \log(N/\psi))$, $\forall i$, *w.h.p.*. The assert follows according to Lemma 1. ■

Theorem 1: For the social-proximity grid-like vehicular networks, with the two-hop relay scheme $\mathcal{X}$, the per-vehicle throughput $\lambda(\Phi)$ cannot be better than $\frac{1}{2\psi\lceil 1+\Delta\rceil\lceil 2+\Delta\rceil}$, and *w.h.p.*, we obtain the following.

i) When $\kappa + \nu > 1$

$$\lambda(\Phi) = \begin{cases} \Omega\left(\frac{1}{\psi(N/\psi)^{\frac{1}{2}\kappa\gamma}}\right), & 0 < \gamma < 2 \\ \Omega\left(\frac{1}{\psi(N/\psi)^{\kappa}\log(N/\psi)}\right), & \gamma = 2, \psi = \Theta(1) \\ \Omega\left(\frac{\log(N/\psi)}{\psi(N/\psi)^{\kappa}}\right), & \gamma = 2, \psi = \omega(1) \\ \Omega\left(\frac{1}{\psi(N/\psi)^{\kappa}}\right), & \gamma > 2. \end{cases}$$

ii) When $\kappa + \nu \leq 1$

a) $\kappa = 0$, $\lambda(\Phi) = \Omega\left(\frac{(N/\psi)^{\nu-1}}{\psi \log(N/\psi)}\right)$;

b) $\kappa \neq 0$

$$\lambda(\Phi) = \begin{cases} \Omega\left(\frac{(N/\psi)^{\nu-\frac{1}{2}\kappa\gamma-1}}{\psi\log(N/\psi)}\right), & 0 < \gamma < 1 \\ \Omega\left(\frac{(N/\psi)^{\nu-\frac{1}{2}\kappa-1}}{\psi}\right), & \gamma = 1 \\ \Omega\left(\frac{(N/\psi)^{\nu-\kappa(1-\frac{1}{2}\gamma)-1}}{\psi\log(N/\psi)}\right), & 1 < \gamma < 2 \\ \Omega\left(\frac{(N/\psi)^{\nu-1}}{\psi\log^2(N/\psi)}\right), & \gamma = 2 \\ \Omega\left(\frac{(N/\psi)^{\nu-1}}{\psi\log(N/\psi)}\right), & \gamma > 2. \end{cases}$$

Proof: The proof consists of two parts. We first apply Lemmas 1 and 3 to derive the lower bound of the per-vehicle throughput. Following the two-hop relay scheme $\mathcal{X}$, the long-term throughput of flow k (denoting the source and destination of flow k by $\mathbb{S}$ and $\mathbb{D}$, respectively) is given by

$$\lambda_k(\Phi) = \lim_{T \to \infty} L_k(T)/T \tag{12}$$

$$= \frac{1}{2} p_{\mathrm{ac}} \sum_{i=1}^{G} \mathbf{Pr}\left(\mathcal{N}_i \geq 2, \mathcal{N}_i^{\mathbb{SD}} = 0 | \mathcal{C}_{\mathbb{D}} = i\right) \pi_{\mathbb{D}}(i) \frac{1}{\mathcal{N}_i} \tag{13}$$

$$+ p_{\mathrm{ac}} \sum_{i=1}^{G} \mathbf{Pr}(\mathcal{C}_{\mathbb{S}} = i | \mathcal{C}_{\mathbb{D}} = i) \pi_{\mathbb{D}}(i) \frac{1}{\mathcal{N}_i^{\mathbb{SD}}} \tag{14}$$

where $\mathcal{N}_i$ and $\mathcal{N}_i^{\mathbb{SD}}$ denote the number of vehicles and the number of $\mathbb{S}$-$\mathbb{D}$ pairs on road segment i in a time-slot, respectively. Recall that $\pi_{\mathbb{D}}(i)$ is the steady-state probability that $\mathbb{D}$ stays on road segment i.

Let $\mathfrak{N}_i$ denote the number of $\mathbb{S}$-$\mathbb{D}$ pairs whose mobility region contains road segment i. The probability of finding at least two vehicles and no $\mathbb{S}$-$\mathbb{D}$ pair on road segment i given that $\mathbb{D}$ is on road segment i is given by, *w.h.p.*, $\forall i$

$$\mathbf{Pr}\left(\mathcal{N}_i \geq 2, \mathcal{N}_i^{\mathbb{SD}} = 0 | \mathcal{C}_{\mathbb{D}} = i\right)$$
$$\geq (1-\pi_1')\left(1 - \left(1 - \frac{2\pi_1'}{\mathcal{A}^\gamma} + 2\left(\frac{\pi_1'}{\mathcal{A}^\gamma}\right)^2\right)^{\mathfrak{N}_i - 1}\right)$$
$$= (1-\pi_1')\left(1 - \left(1 + \left(-\frac{\mathcal{A}^\gamma}{2\pi_1'}\right)^{-1} + \frac{1}{2}\left(-\frac{\mathcal{A}^\gamma}{2\pi_1'}\right)^{-2}\right)^{-\frac{\mathcal{A}^\gamma}{2\pi_1'}(-2\mathfrak{N}_i\mathcal{A}^{-\gamma}\pi_1' + 2\mathcal{A}^{-\gamma}\pi_1')}\right)$$
$$\geq (1-\pi_1')\left(1 - \left(\left(1 + \frac{1}{\mathscr{Z}} + \frac{1}{2\mathscr{Z}^2}\right)^{\mathscr{Z}}\right)^{-\underline{d}_i^N - 1/\mathscr{Z}}\right)$$

where we denote $-\mathcal{A}^\gamma/(2\pi_1')$ by $\mathscr{Z}$. If $\underline{d}_i^N = \omega(1)$, $((1+1/\mathscr{Z} + 1/(2\mathscr{Z}^2))^{\mathscr{Z}})^{-\underline{d}_i^N - 1/\mathscr{Z}} \to 0$, as $N \to \infty$. Therefore, the event "$\mathcal{N}_i \geq 2, \mathcal{N}_i^{\mathbb{SD}} = 0 | \mathcal{C}_{\mathbb{D}} = i$" holds *w.h.p.* when $\gamma \leq 2$, and at least with a constant probability $1 - \pi_1'$ when $\gamma > 2$, according to Lemma 1. If $\underline{d}_i^N = \Theta(1)$, $\mathbf{Pr}(\mathcal{N}_i \geq 2, \mathcal{N}_i^{\mathbb{SD}} = 0 | \mathcal{C}_{\mathbb{D}} = i)$ is lower-bounded by $(1-\pi_1')(1 - e^{-\underline{d}_i^N})$. If $\underline{d}_i^N = o(1)$, $\mathbf{Pr}(\mathcal{N}_i \geq 2, \mathcal{N}_i^{\mathbb{SD}} = 0 | \mathcal{C}_{\mathbb{D}} = i) \to 0$, as $N \to \infty$.

According to the results of partial sum of p-series, the probability of finding $\mathbb{S}$ and $\mathbb{D}$ on a same road segment during a slot is asymptotically given by

$$\sum_{i=1}^{G} \mathbf{Pr}(\mathcal{C}_{\mathbb{S}} = i | \mathcal{C}_{\mathbb{D}} = i) \pi_{\mathbb{D}}(i)$$
$$= \sum_{i=1}^{G} \pi_{\mathbb{S}}(i)\pi_{\mathbb{D}}(i) = \sum_{\alpha=1}^{\mathcal{A}} (16\alpha - 12)\alpha^{-2\gamma}\pi_1'^2$$
$$= \pi_1'^2 \sum_{\alpha=1}^{\mathcal{A}} \left(\frac{16}{\alpha^{2\gamma-1}} - \frac{12}{\alpha^{2\gamma}}\right)$$
$$= \begin{cases} \Theta\left(\pi_1'^2 (N/\psi)^{\kappa(1-\gamma)}\right), & 0 < \gamma < 1 \\ \Theta\left(\pi_1'^2 \log(N/\psi)\right), & \gamma = 1 \\ \Theta\left(\pi_1'^2\right), & \gamma > 1. \end{cases} \tag{15}$$

Based on the analysis above, when $\underline{d}_i^N = \Omega(1)$, $\forall k$, *w.h.p.* we have

$$\lambda_k(\Phi) \geq \frac{c' p_{\mathrm{ac}}}{2\overline{d}_i^N} \sum_{i=1}^{G} \pi_{\mathbb{D}}(i) + \frac{p_{\mathrm{ac}}}{\overline{d}_i^N} \sum_{i=1}^{G} \pi_{\mathbb{S}}(i)\pi_{\mathbb{D}}(i)$$
$$= c' p_{\mathrm{ac}}/\overline{d}_i^N + O(1) p_{\mathrm{ac}}/\overline{d}_i^N$$

where c' is constant. Therefore, $\lambda(\Phi) = \Omega\left(p_{\rm ac}/\overline{d}_i^N\right)$, *w.h.p.* When $\underline{d}_i^N = o(1)$, $\forall k$, $\lambda_k(\Phi) \geq p_{\rm ac}(\sum_{i=1}^{G}\pi_{\mathbb{S}}(i)\pi_{\mathbb{D}}(i))/\overline{d}_i^N$. Thus, *w.h.p.*, we have $\lambda(\Phi) = \Omega\left(p_{\rm ac}\left(\sum_{i=1}^{G}\pi_{\mathbb{S}}(i)\pi_{\mathbb{D}}(i)\right)/\overline{d}_i^N\right)$. From Lemmas 1 and 3, the assert follows.

Next, we derive an upper bound of per-vehicle throughput considering any possible stabilizing scheduling policies under $\mathcal{X}$-I. Let $\mathscr{X}_d(T)$ denote the number of packets delivered in the network through direct transmissions from the source to destination, and $\mathscr{X}_r(T)$ denote the number of packets delivered to the destination via relaying, during the interval $[0,T]$. Therefore, provided the arbitrary and fixed $\epsilon > 0$, there must exist arbitrarily large values of T such that the per-vehicle throughput $\lambda(\Phi)$ satisfies

$$\frac{\mathscr{X}_d(T)+\mathscr{X}_r(T)}{T} \geq N\lambda(\Phi) - \epsilon. \tag{16}$$

Let $\mathscr{Y}(T)$ denote the total number of transmission opportunities during the interval $[0,T]$. From (16), we have

$$\begin{aligned}\frac{1}{T}\mathscr{Y}(T) &\geq \frac{1}{T}\mathscr{X}_d(T) + \frac{2}{T}\mathscr{X}_r(T)\\ &\geq \frac{1}{T}\mathscr{X}_d(T) + 2\left((N\lambda(\Phi)-\epsilon) - \frac{1}{T}\mathscr{X}_d(T)\right).\end{aligned}$$

The first inequality holds because the relayed packet reaches to the destination through at least two hops. Therefore

$$\lambda(\Phi) \leq \frac{\frac{1}{T}\mathscr{Y}(T) + \frac{1}{T}\mathscr{X}_d(T) + 2\epsilon}{2N}$$

i.e.,

$$\lambda(\Phi) \leq \lim_{T\to\infty}\frac{\frac{1}{T}\mathscr{Y}(T) + \frac{1}{T}\mathscr{X}_d(T)}{2N}. \tag{17}$$

Due to the interference of transmissions, the total number of transmission opportunities is no larger than the maximum number of concurrent transmissions during $[0,T]$. We have $\lim_{T\to\infty}\frac{1}{T}\mathscr{Y}(T) \leq Gp_{\rm ac}$. Similarly, we have $\lim_{T\to\infty}\frac{1}{T}\mathscr{X}_d(T) \leq Gp_{\rm ac}$, where the equality holds when there is always an $\mathbb{S}$-$\mathbb{D}$ transmission on each road segment of a noninterference group during each time-slot. By plugging the inequalities into (17), we have

$$\lambda(\Phi) \leq \frac{Gp_{\rm ac}+Gp_{\rm ac}}{2N} = \frac{p_{\rm ac}}{\psi} = \Theta\left(\frac{1}{\psi}\right). \tag{18}$$

From (18), $\lambda(\Phi)$ cannot be better than $\Theta\left(\frac{1}{\psi}\right)$. ∎

C. Average Per-Vehicle Throughput

We derive a lower bound of the average per-vehicle throughput $\widetilde{\lambda}(\Phi)$, stated in Theorem 2, based on the proposed two-hop relay scheme for $\gamma \geq 2$, where the network shows dramatic social features. To simplify the analysis, we let $\psi = \Theta(1)$ in this section, i.e., the network density keeps constant and does not scale up with the population of vehicles. Considering all possible functions of ψ with the order of $o(N)$ makes the derivation very complicated. The following lemmas (Lemmas 4–8) will be first presented to prove Theorem 2.

Lemma 4: Let $\mathscr{T}$ be a regular tessellation of the network, whose elements $\mathscr{T}_i$ contain $\lceil 100N^{1-\nu}\log(N)\rceil$ street blocks. *W.h.p.*, every element of $\mathscr{T}$ contains at least one social spot.

Proof: Recall that each element $\mathscr{T}_i$ of $\mathscr{T}$ is a regular area containing $\lceil 100N^{1-\nu}\log(N)\rceil$ street blocks. Let $\mathscr{T}_i^{\rm s}$ denote the number of social spots contained in $\mathscr{T}_i$. Applying the Vapnik–Chervonenkis Theorem, $\forall\mathscr{T}_i$

$$\mathbf{Pr}\left\{\sup_{\mathscr{T}_i\in\mathscr{T}}\left|\frac{\mathscr{T}_i^{\rm s}}{V} - \frac{100N^{1-\nu}\log(N)}{C}\right| \leq \epsilon\right\} > 1-\delta.$$

Note that VC-d($\mathscr{T}$) is at most 4. The condition (10) is satisfied when $\epsilon = \delta = \frac{50\log(N)}{N^\nu}$. Therefore, $\forall\mathscr{T}_i$

$$\mathbf{Pr}\{\mathscr{T}_i^{\rm s} \geq 50\log(N)\} > 1 - \frac{50\log(N)}{N^\nu}.$$

The lemma follows as $N\to\infty$. ∎

We denote by $P(\Phi) = E\left[\sum_{i=1}^{G}\mathbb{1}_{\mathcal{N}_i\geq 2}\right]$ the average number of road segments where there are at least two vehicles during a time-slot. Similarly, let $Q(\Phi) = E\left[\sum_{i=1}^{G}\mathbb{1}_{\mathcal{N}_i^{\mathbb{SD}}\geq 1}\right]$ denote the average number of road segments where there is at least one $\mathbb{S}$-$\mathbb{D}$ pair during a time-slot. Lemmas 5 and 8 present a lower bound of $P(\Phi)$.

Lemma 5: When $\nu \neq 1$, *w.h.p.*, we have

$$P(\Phi) = \begin{cases}\Omega\left(N^{\frac{2}{\gamma}+\nu(1-\frac{2}{\gamma})}/\log^3(N)\right), & \kappa+\nu>1\\ \Omega\left(N^{\nu+\frac{2\kappa}{\gamma}}/\log(N)\right), & \kappa+\nu<1\\ \Omega\left(N^{\nu+\frac{2\kappa}{\gamma+\vartheta}}/\log(N)\right), & \kappa+\nu=1\end{cases}$$

where ϑ is a positive and arbitrarily small value.

Proof: We consider a single social spot S_j in an area. Recall that S_j^v is the number of vehicles associated with S_j. For road segment i in the mobility region of the vehicles, from (8), we have

$$\begin{aligned}\mathbf{Pr}(\mathcal{N}_i\geq 2) &= 1-\mathbf{Pr}(\mathcal{N}_i\leq 1)\\ &\geq 1-(1-\pi'_{\mathcal{B}})^{\frac{(1-\varepsilon)N}{V}} - \frac{(1-\varepsilon)N}{V}\pi'_{\mathcal{B}}(1-\pi'_{\mathcal{B}})^{\frac{(1-\varepsilon)N}{V}-1}\\ &\geq 1-e^{-\pi'_{\mathcal{B}}\frac{(1-\varepsilon)N}{V}} - \pi'_{\mathcal{B}}\frac{(1-\varepsilon)N}{V}e^{-\pi'_{\mathcal{B}}\frac{(1-\varepsilon)N}{V}+\pi'_{\mathcal{B}}}\\ &= 1-e^{-\pi'_{\mathcal{B}}\frac{(1-\varepsilon)N}{V}}\left(1+\pi'_{\mathcal{B}}\frac{(1-\varepsilon)N}{V}e^{\pi'_{\mathcal{B}}}\right)\end{aligned}$$

where $\pi'_{\mathcal{B}} = \mathcal{B}^{-\gamma}\pi'_1$ and $\mathcal{B} \leq \min\left\{\mathcal{A}, \lceil 10\sqrt{N^{1-\nu}\log(N)}\rceil\right\}$ from Lemma 4. Furthermore, it is satisfied that $\pi'_{\mathcal{B}}\frac{N}{V} = \omega(1)$. Therefore, letting $\varepsilon\to 0$, as $\to\infty$, the event "$\mathcal{N}_i \geq 2$" holds *w.h.p.* Considering the regular tessellation $\mathscr{T}$ of the network, according to Lemma 4, *w.h.p.*, we have

$$\begin{aligned}P(\Phi) &= \sum_{i=1}^{G}E[\mathbb{1}_{\mathcal{N}_i\geq 2}] = \sum_{i=1}^{G}\mathbf{Pr}(\mathcal{N}_i\geq 2)\\ &\geq \frac{C}{100N^{1-\nu}\log(N)}\cdot\frac{1}{4}\cdot 4\mathcal{B}(2\mathcal{B}-1)\\ &= \Theta\left(\frac{\mathcal{B}^2N^\nu}{\log(N)}\right).\end{aligned} \tag{19}$$

This article has been accepted for inclusion in a future issue of this journal. Content is final as presented, with the exception of pagination.

For $\kappa+\nu>1$, we choose $\mathcal{B}=\Theta(N^{\frac{1-\nu}{\gamma}}/\log(N))$. $\mathcal{B}$ can scale as $\Theta(N^{\frac{\kappa}{\gamma+\vartheta}})$ for $\kappa+\nu=1$. When $\kappa+\nu<1$, $\mathcal{B}$ can be $\Theta(N^{\frac{\kappa}{\gamma}})$. The lemma follows. ■

Lemma 6 (Chebyshev's Inequality): If X is a random variable with mean $E[X]$ and variance $\mathrm{Var}(X)$, then for any value $k>0$

$$\mathbf{Pr}(\mid X-E[X]\mid\geq k)\leq\frac{\mathrm{Var}(X)}{k^2}.$$

Lemma 6 is well known, and we will use it to prove Lemma 7.

Lemma 7: When $\nu=1$, at least $(1-e^{-\psi})C$ social spots will associate with at least one $\mathbb{S}$-$\mathbb{D}$ pair *w.h.p.*

Proof: We denote by $\mathbb{1}_C=\sum_{i=1}^{C}\mathbb{1}_{S_i^v=0}$ the number of social spots that are not chosen by any $\mathbb{S}$-$\mathbb{D}$ pair in the network. $\mathbf{Pr}(\mathbb{1}_{S_i^v=0}=1)=(1-\frac{1}{C})^{\frac{N}{2}}$. Thus, the expectation and variance of $\mathbb{1}_{S_i^v=0}$ are $E[\mathbb{1}_{S_i^v=0}]=(1-\frac{1}{C})^{\frac{N}{2}}$ and $\mathrm{Var}(\mathbb{1}_{S_i^v=0})=(1-\frac{1}{C})^{\frac{N}{2}}-(1-\frac{1}{C})^{N}$, respectively. Next, we need to determine the variance of $\mathbb{1}_C$. For any $i\neq j$, $j\in\{1,2,\ldots,C\}$, $\mathrm{Cov}(\mathbb{1}_{S_i^v=0},\mathbb{1}_{S_j^v=0})=E[\mathbb{1}_{S_i^v=0}\mathbb{1}_{S_j^v=0}]-E[\mathbb{1}_{S_i^v=0}]E[\mathbb{1}_{S_j^v=0}]$, where $\mathrm{Cov}(\mathbb{1}_{S_i^v=0},\mathbb{1}_{S_j^v=0})$ is the covariance of variable $\mathbb{1}_{S_i^v=0}$ and $\mathbb{1}_{S_j^v=0}$. It is easy to get that $E[\mathbb{1}_{S_i^v=0}\mathbb{1}_{S_j^v=0}]=(1-\frac{2}{C})^{\frac{N}{2}}$. Since $\mathrm{Cov}(\mathbb{1}_{S_i^v=0},\mathbb{1}_{S_i^v=0})=\mathrm{Var}(\mathbb{1}_{S_i^v=0})$, we have

$$\begin{aligned}\mathrm{Var}(\mathbb{1}_C)&=\mathrm{Var}\left(\sum_{i=1}^{C}\mathbb{1}_{S_i^v=0}\right)\\&=\sum_{i=1}^{C}\sum_{j=1}^{C}\mathrm{Cov}\left(\mathbb{1}_{S_i^v=0},\mathbb{1}_{S_j^v=0}\right)\\&=\sum_{i=1}^{C}\mathrm{Cov}\left(\mathbb{1}_{S_i^v=0},\mathbb{1}_{S_i^v=0}\right)\\&\quad+2\sum_{i=1}^{C}\sum_{j<i}\mathrm{Cov}\left(\mathbb{1}_{S_i^v=0},\mathbb{1}_{S_j^v=0}\right)\\&=C\left(\left(1-\frac{1}{C}\right)^{\frac{N}{2}}-\left(1-\frac{1}{C}\right)^{N}\right)\\&\quad+C(C-1)\left(\left(1-\frac{2}{C}\right)^{\frac{N}{2}}-\left(1-\frac{1}{C}\right)^{N}\right)\\&\leq C\left(\left(1-\frac{1}{C}\right)^{\frac{N}{2}}-\left(1-\frac{1}{C}\right)^{N}\right).\end{aligned}$$

The inequality holds because $\left(1-\frac{2}{C}\right)^{\frac{N}{2}}-\left(1-\frac{1}{C}\right)^{N}=\left(1-\frac{2}{C}\right)^{\frac{N}{2}}-\left(1-\frac{2}{C}+\frac{1}{C^2}\right)^{\frac{N}{2}}\leq 0$. From Lemma 6, choosing $k=\epsilon C$, we have

$$\mathbf{Pr}(\mathbb{1}_C-E[\mathbb{1}_C]\geq\epsilon C)\leq\frac{C\left[\left(1-\frac{1}{C}\right)^{\frac{N}{2}}-\left(1-\frac{1}{C}\right)^{N}\right]}{\epsilon^2C^2}.$$

Note that $E[\mathbb{1}_C]=C\left(1-\frac{1}{C}\right)^{\frac{N}{2}}$. Thus

$$\mathbf{Pr}\left(\frac{\mathbb{1}_C}{C}\geq(\rho+\epsilon)\right)\leq\frac{\rho-\rho^2}{\epsilon^2}\cdot\frac{1}{C},$$

where $\rho=\left(1-\frac{1}{C}\right)^{\frac{N}{2}}$. Since $N=2\psi C$, as $N\to\infty$, $\rho\to e^{-\psi}$. Therefore, $\lim_{N\to\infty}\mathbf{Pr}(\mathbb{1}_C/C\geq e^{-\psi})=0$, i.e., the probability of $\mathbb{1}_C$ being over a constant proportion of C goes to zero as $N\to\infty$. The lemma follows. ■

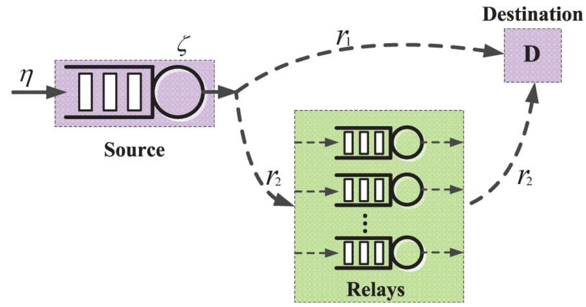

Fig. 9. A decoupling queue structure.

Lemma 8: When $\nu=1$, *w.h.p.*, $P(\Phi)=\Omega\left(N/\log^2(N)\right)$ for $\gamma=2$ and $\kappa\neq 0$; $P(\Phi)=\Theta(N)$ for $\gamma=2$ and $\kappa=0$; $P(\Phi)=\Theta(N)$ for $\gamma>2$.

Proof: According to Lemma 7, we can obtain that *w.h.p.*, there are at least $2(1-e^{-\psi})C$ road segments, each of which belongs to a $\mathrm{Tier}(1)$ of vehicles' mobility region. Let $\mathcal{S}$ denote the set of road segments that are not contained in the mobility region of any vehicle. $\bar{\mathcal{S}}$ is the complementary set of $\mathcal{S}$ in $\{1,2,\ldots,G\}$. Note that $\mathbf{Pr}(\mathcal{N}_i\geq 2)=0$, $\forall i\in\mathcal{S}$. Thus

$$\begin{aligned}P(\Phi)&=\sum_{i=1}^{G}E[\mathbb{1}_{\mathcal{N}_i\geq 2}]=\sum_{i=1}^{G}\mathbf{Pr}(\mathcal{N}_i\geq 2)\\&=\sum_{i\in\mathcal{S}}\mathbf{Pr}(\mathcal{N}_i\geq 2)+\sum_{j\in\bar{\mathcal{S}}}\mathbf{Pr}(\mathcal{N}_j\geq 2)\\&=|\mathcal{S}|\cdot 0+\sum_{j\in\bar{\mathcal{S}}}\mathbf{Pr}(\mathcal{N}_j\geq 2)\geq\sum_{j\in\bar{\mathcal{S}}}\pi_1'^2\end{aligned}$$

since for any $j\in\bar{\mathcal{S}}$, $\mathbf{Pr}(\mathcal{N}_j\geq 2)\geq\pi_1'^2$. The lemma follows from Lemma 7. ■

Theorem 2: For the social-proximity grid-like vehicular networks, with the two-hop relay scheme $\mathcal{X}$, a bound of average per-vehicle throughput capacity $\widetilde{\lambda}(\Phi)$ is given by *w.h.p.*:

i) when $\nu\neq 1$ and $\gamma\geq 2$

$$\widetilde{\lambda}(\Phi)=\begin{cases}\Omega\left(N^{\frac{2}{\gamma}+\nu(1-\frac{2}{\gamma})-1}/\log^3(N)\right), & \kappa+\nu>1\\\Omega\left(N^{\nu+\frac{2\kappa}{\gamma+\vartheta}-1}/\log(N)\right), & \kappa+\nu=1\\\Omega\left(N^{\nu+\frac{2\kappa}{\gamma}-1}/\log(N)\right), & \kappa+\nu<1;\end{cases}$$

ii) when $\nu=1$, $\widetilde{\lambda}(\Phi)=\Omega\left(\frac{1}{\log^2(N)}\right)$, for $\gamma=2$ and $\kappa\neq 0$; $\widetilde{\lambda}(\Phi)=\Theta(1)$ for $\gamma=2$ and $\kappa=0$; $\widetilde{\lambda}(\Phi)=\Theta(1)$ for $\gamma>2$.

Proof: Based on the two-hop relay scheme $\mathcal{X}$, we are able to use a decoupling queue structure, similar to that in [8], to model each unicast flow, as shown in Fig. 9. Without loss of generality, we consider that the packet arrival rate η follows the Bernoulli process. In other words, in each unicast flow, one packet arrives with the probability η at the current slot, and with the rest probability if there is no packet arrival. Therefore, the source vehicle, e.g., v_k, can be represented as a Bernoulli/Bernoulli queue with packet arrival rate η_k and service rate ζ_k. The buffering packet in the source will be transmitted (served) to either its destination directly or one of the relays within the mobility region of the source. The transmission opportunity arises with probability ζ_k. Let $r_1^k(N)$

denote the long-term average rate at which a direct transmission to the destination is scheduled to source v_k, and $r_2^k(N)$ denote the long-term average rate at which a source-to-relay transmission is scheduled to source v_k. The transmission opportunity arises at the rate $\zeta_k(N) = r_1^k(N) + r_2^k(N)$. As per the definition, $\widetilde{\lambda}(\Phi) = \frac{\sum_{k=1}^N \zeta_k(N)}{N}$. Since the two-hop relay scheme $\mathcal{X}$ schedules a source-to-relay transmission and a relay-to-destination transmission equally likely, the rate into the relays is equal to the rate out of the relays. During each time-slot, the total number of transmission opportunities over the network is $\sum_{k=1}^N (r_1^k(N) + 2r_2^k(N))$. Given that the transmission opportunity arises on a road segment when it is active and at least two vehicles are on it, then we have

$$p_{\mathrm{ac}} P(\Phi) = \sum_{k=1}^{N} \left(r_1^k(N) + 2r_2^k(N) \right). \tag{20}$$

Since the two-hop relay scheme $\mathcal{X}$ schedules the source-to-destination transmission whenever possible, then we have

$$p_{\mathrm{ac}} Q(\Phi) = \sum_{k=1}^{N} r_1^k(N). \tag{21}$$

From (20) and (21), we obtain $\sum_{k=1}^N r_2^k(N) = \frac{p_{\mathrm{ac}}(P(\Phi)-Q(\Phi))}{2}$, and therefore

$$\widetilde{\lambda}(\Phi) = \frac{\sum\limits_{k=1}^{N} \left(r_1^k(N) + r_2^k(N) \right)}{N} = \frac{p_{\mathrm{ac}}(P(\Phi)+Q(\Phi))}{2N}.$$

Since $P(\Phi) \geq Q(\Phi)$ and from Lemmas 5 and 8, the theorem follows. ■

Remark: The average per-vehicle throughput is analyzed as a global metric to evaluate the network performance with inhomogeneous vehicle density. For example, from Theorem 2, we can attain that the constant per-vehicle throughput is feasible w.h.p. for N_f $\mathbb{S}$-$\mathbb{D}$ pairs, where $N_f = \Theta(N) \leq \frac{N}{2}$, when $\nu = 1$ and $\gamma > 2$. Because of the socialized mobility of vehicles and the randomness of the locations of vehicle's social spots, the network shows spatial variations of vehicle density. Therefore, the throughput performance of vehicles in different areas of the city grid may be different. For example, in a hot area covered by a large number of different overlapped mobility regions, the throughput of an $\mathbb{S}$-$\mathbb{D}$ pair in that area may drop significantly.

D. Average Packet Delay

We first analyze the average packet delay of a given unicast flow. The packet delay is accounted starting from the time-slot when the packet arrives at the source until the time-slot when the packet is delivered to its destination (including the queueing delay at the source or relay vehicle).

Recall that the source v_k can be represented as a Bernoulli/Bernoulli queue with arrival rate η_k and service rate ζ_k. The expected number of packets buffered at the source is

$$E_k[n_s] = \frac{\eta_k(1-\eta_k)}{\zeta_k - \eta_k}. \tag{22}$$

It has been shown in [8] that packets depart from the source at the rate of η_k when the buffer of the source is stable. For a packet from the source, it is delivered to a relay vehicle, e.g., v_i, with the probability $\frac{r_2^k}{\zeta_k} \cdot P_{ki}$, where P_{ki} is the contact probability between v_k and v_i. Therefore, the packet arrival rate to the relay v_i is $\eta_{ki} = \frac{\eta_k r_2^k}{\zeta_k} P_{ki}$. The packets depart to the destination from the relay v_i at the rate $\zeta_{ki} = r_2^k P_{ki}$. This is because the source and the destination have the equal contact probability with the relay vehicles, and moreover the packet injection rate from the source to the relays equals that from the relays to the destination, as shown in Fig. 9. With the packet arrivals and departures at the relay v_i following the Bernoulli process with mean rates η_{ki} and ζ_{ki}, respectively, the average number of packets held by v_i is

$$E_{ki}[n_r] = \frac{\eta_{ki}}{\zeta_{ki} - \eta_{ki}} = \frac{\eta_k}{\zeta_k - \eta_k}. \tag{23}$$

Note that (23) holds for every relay. From Little's law, the average packet delay of the flow from v_k is

$$\mathcal{D}_k(N) = \frac{E_k[n_s] + R_k(N) E_{ki}[n_r]}{\eta_k} = \frac{R_k(N) + 1 - \eta_k}{\zeta_k - \eta_k} \tag{24}$$

where $R_k(N)$ is the total number of relay vehicles that have an overlapped mobility region with source v_k. As indicated by (24), the average packet delay is dependent of vehicle density in the proximity region of a unicast flow.

We proceed to derive the lower bound and upper bound of the average packet delay of the entire network. We neglect the queueing delay at the source vehicle and the propagation delay in the calculation, as we are only interested in the packet delay caused by vehicles' mobility.

Theorem 3: For the social-proximity grid-like vehicular networks, with the two-hop relay scheme $\mathcal{X}$, *w.h.p.*, we obtain the following bounds of the average packet delay $\mathcal{D}(N)$.

i) When $\kappa + \nu > 1$

$$\mathcal{D}(\Phi) = O\left(\psi^2 (N/\psi)^{\kappa(2+\gamma)} \right).$$

ii) When $\kappa + \nu \leq 1$

$$\mathcal{D}(\Phi) = O\left(\frac{\psi^2 \log^2(N/\psi)}{(N/\psi)^{2(\nu-1)-\kappa\gamma}} \right).$$

iii) $\mathcal{D}(\Phi) = \Omega((N/\psi)^{\kappa})$, for $0 < \gamma < 1$; $\mathcal{D}(\Phi) = \Omega((N/\psi)^{\kappa}/\log(N/\psi))$, for $\gamma = 1$; $\mathcal{D}(\Phi) = \Omega((N/\psi)^{\kappa(2-\gamma)})$, for $1 < \gamma < 2$; $\mathcal{D}(\Phi) = \Omega(\log^2(N/\psi))$, for $\gamma = 2$; $\mathcal{D}(\Phi) = \Omega(1)$, for $\gamma > 2$.

Proof: The minimal delay of a flow is achieved when the source delivers the flow packets to its destination with the highest transmission priority. Moreover, the direct packet transmission from the source to the destination has lower average delay compared to the relay transmissions, with the condition that the contact probability between the source and one of its relay vehicles is no larger than the contact probability between the source and its destination. The source encounters the destination on the same road segment with the probability

$$P_{\mathbb{S}\mathbb{D}} = \sum_{i=1}^{G} \pi_{\mathbb{S}}(i) \pi_{\mathbb{D}}(i).$$

Therefore, the minimum packet delay is geometric distributed with mean $1/P_{\mathbb{S}\mathbb{D}}$. According to (15), we obtain a lower bound of $\mathcal{D}(\Phi)$.

Next, we derive an upper bound of the average packet delay. Let v_A and v_B be a given pair of vehicles whose mobility regions are overlapped. v_A intends to transmit a packet to v_B. The transmission between v_A and v_B can be scheduled during a time-slot only when the following three events occur at the same time: 1) v_A and v_B are located on the same road segment during the time-slot; 2) that road segment is active in the slot; and 3) v_A and v_B are both selected for a transmission from v_A to v_B. These three events occur with probability ϕ_1, p_{ac} and ϕ_2, respectively. Thus, the distribution of the packet delay between v_A and v_B can be treated as geometric with mean

$$\frac{1}{\phi_1 \phi_2 p_{\mathrm{ac}}} = O\left(\left(\frac{\mathcal{A}^{\gamma}}{\pi_1'}\overline{d}_i^N\right)^2\right)$$

where ϕ_1 cannot be lower than $(\mathcal{A}^{-\gamma}\pi_1')^2$ and ϕ_2 is $\Omega\left(1/\left(\overline{d}_i^N\right)^2\right)$. From Lemma 3, we can attain an upper bound of $\mathcal{D}(\Phi)$. The theorem follows. ■

VI. Conclusion

In this paper, we have investigated the asymptotic capacity and delay performance for social-proximity vehicular networks. We adopt a scalable city grid to deploy the vehicular network and consider a socialized mobility model for each vehicle. The user applications have proximity nature, i.e., the source and the destination of each flow have an identical social spot. With the proposed two-hop relay scheme, the bounds of the per-vehicle throughput capacity, average per-vehicle throughput, and average packet delay have been derived with respect to different network parameters. We have shown that the asymptotic performance limits of the network highly depend on the inherent parameters of mobility patterns. Our results can be applied to predict the network performance and provide guidance on the design and implementations for large-scale vehicular networks. Our future work includes extensive simulation validations base on the trace data of real-world scenarios and packet forwarding protocol design for the social-proximity vehicular network.

References

[1] D. Jiang, V. Taliwal, A. Meier, W. Holfelder, and R. Herrtwich, "Design of 5.9 GHz DSRC-based vehicular safety communication," *IEEE Wireless Commun.*, vol. 13, no. 5, pp. 36–43, Oct. 2006.

[2] F. Bai and B. Krishnamachari, "Exploiting the wisdom of the crowd: localized, distributed information-centric VANETs," *IEEE Commun. Mag.*, vol. 48, no. 5, pp. 138–146, May 2010.

[3] T. Luan, L. Cai, J. Chen, X. Shen, and F. Bai, "VTube: Towards the media rich city life with autonomous vehicular content distribution," in *Proc. IEEE SECON*, Salt Lake City, UT, USA, Jun. 2011, pp. 359–367.

[4] R. Lu, X. Lin, T. Luan, X. Liang, and X. Shen, "Pseudonym changing at social spots: An effective strategy for location privacy in VANETs," *IEEE Trans. Veh. Technol.*, vol. 61, no. 1, pp. 86–96, Jan. 2012.

[5] Z. Wang, L. Liu, M. Zhou, and N. Ansari, "A position-based clustering technique for ad hoc intervehicle communication," *IEEE Trans. Syst., Man, Cybern. C, Appl. Rev.*, vol. 38, no. 2, pp. 201–208, Mar. 2008.

[6] N. Sarafijanovic-Djukic, M. Pidrkowski, and M. Grossglauser, "Island hopping: Efficient mobility-assisted forwarding in partitioned networks," in *Proc. IEEE SECON*, Reston, VA, USA, Sep. 2006, vol. 1, pp. 226–235.

[7] P. Li, M. Pan, and Y. Fang, "The capacity of three-dimensional wireless ad hoc networks," in *Proc. IEEE INFOCOM*, Shanghai, China, Apr. 2011, pp. 1485–1493.

[8] M. Neely and E. Modiano, "Capacity and delay tradeoffs for ad hoc mobile networks," *IEEE Trans. Inf. Theory*, vol. 51, no. 6, pp. 1917–1937, Jun. 2005.

[9] P. Gupta and P. Kumar, "The capacity of wireless networks," *IEEE Trans. Inf. Theory*, vol. 46, no. 2, pp. 388–404, Mar. 2000.

[10] X. Li, "Multicast capacity of wireless ad hoc networks," *IEEE/ACM Trans. Netw.*, vol. 17, no. 3, pp. 950–961, Jun. 2009.

[11] J. Ghaderi, L. Xie, and X. Shen, "Hierarchical cooperation in ad hoc networks: Optimal clustering and achievable throughput," *IEEE Trans. Inf. Theory*, vol. 55, no. 8, pp. 3425–3436, Aug. 2009.

[12] M. Grossglauser and D. Tse, "Mobility increases the capacity of ad hoc wireless networks," *IEEE/ACM Trans. Netw.*, vol. 10, no. 4, pp. 477–486, Aug. 2002.

[13] L. Ying, S. Yang, and R. Srikant, "Optimal delay-throughput tradeoffs in mobile ad hoc networks," *IEEE Trans. Inf. Theory*, vol. 54, no. 9, pp. 4119–4143, Sep. 2008.

[14] A. E. Gamal, J. Mammen, B. Prabhakar, and D. Shah, "Optimal throughput-delay scaling in wireless networks—Part I: The fluid model," *IEEE Trans. Inf. Theory*, vol. 52, no. 6, pp. 2568–2592, Jun. 2006.

[15] X. Lin, G. Sharma, R. Mazumdar, and N. Shroff, "Degenerate delay-capacity tradeoffs in ad-hoc networks with Brownian mobility," *IEEE Trans. Inf. Theory*, vol. 52, no. 6, pp. 2777–2784, Jun. 2006.

[16] K. Lee, Y. Kim, S. Chong, I. Rhee, and Y. Yi, "Delay-capacity tradeoffs for mobile networks with Lévy walks and Lévy flights," in *Proc. IEEE INFOCOM*, 2011, pp. 3128–3136.

[17] P. Li, Y. Fang, and J. Li, "Throughput, delay, and mobility in wireless ad hoc networks," in *Proc. IEEE INFOCOM*, San Diego, CA, USA, Mar. 2010, pp. 1–9.

[18] M. Garetto and E. Leonardi, "Restricted mobility improves delay-throughput tradeoffs in mobile ad hoc networks," *IEEE Trans. Inf. Theory*, vol. 56, no. 10, pp. 5016–5029, Oct. 2010.

[19] D. Ciullo, V. Martina, M. Garetto, and E. Leonardi, "Impact of correlated mobility on delay-throughput performance in mobile ad-hoc networks," in *Proc. IEEE INFOCOM*, San Diego, CA, USA, Mar. 2010, pp. 1–9.

[20] H. Pishro-Nik, A. Ganz, and D. Ni, "The capacity of vehicular ad hoc networks," in *Proc. Allerton Conf.*, 2007, pp. 1156–1163.

[21] M. Nekoui, A. Eslami, and H. Pishro-Nik, "Scaling laws for distance limited communications in vehicular ad hoc networks," *Proc. IEEE ICC*, pp. 2253–2257, 2008.

[22] H. Nishiyama, T. Ngo, N. Ansari, and N. Kato, "On minimizing the impact of mobility on topology control in mobile ad hoc networks," *IEEE Trans. Wireless Commun.*, vol. 11, no. 3, pp. 1158–1166, Mar. 2012.

[23] C. Wang, C. Jiang, X. Li, S. Tang, and P. Yang, "General capacity scaling of wireless networks," in *Proc. IEEE INFOCOM*, Shanghai, China, Apr. 2011, pp. 712–720.

[24] M. Wang, H. Shan, L. Cai, N. Lu, X. Shen, and F. Bai, "Throughput capacity of VANETs by exploiting mobility diversity," in *Proc. IEEE ICC*, Ottawa, ON, Canada, Jun. 2012, pp. 4980–4984.

[25] G. Zhang, Y. Xu, X. Wang, X. Tian, J. Liu, X. Gan, H. Yu, and L. Qian, "Multicast capacity for hybrid VANETs with directional antenna and delay constraint," *IEEE J. Sel. Areas Commun.*, vol. 30, no. 4, pp. 818–833, May 2012.

[26] N. Lu, T. Luan, M. Wang, X. Shen, and F. Bai, "Capacity and delay analysis for social-proximity urban vehicular networks," in *Proc. IEEE INFOCOM*, Orlando, FL, USA, Mar. 2012, pp. 1476–1484.

[27] S. Kostof and R. Tobias, *The City Shaped*. London, U.K.: Thames & Hudson, 1991.

[28] A. Siksna, "The effects of block size and form in North American and Australian city centres," *Urban Morphol.*, vol. 1, pp. 19–33, 1997.

[29] M. Neely, E. Modiano, and C. Rohrs, "Dynamic power allocation and routing for time-varying wireless networks," *IEEE J. Sel. Areas Commun.*, vol. 23, no. 1, pp. 89–103, Jan. 2005.

[30] R. Urgaonkar and M. Neely, "Network capacity region and minimum energy function for a delay-tolerant mobile ad hoc network," *IEEE/ACM Trans. Netw.*, vol. 19, no. 4, pp. 1137–1150, Aug. 2011.

[31] D. Slaughter, *Difference Equations to Differential Equations*. Gainesville, FL, USA: Univ. Press Florida, 2009.

[32] M. Garetto, P. Giaccone, and E. Leonardi, "Capacity scaling in ad hoc networks with heterogeneous mobile nodes: the super-critical regime," *IEEE/ACM Trans. Netw.*, vol. 17, no. 5, pp. 1522–1535, Oct. 2009.

[33] R. Motwani and P. Raghavan, *Randomized Algorithms*. London, U.K.: Chapman & Hall/CRC, 2010.
[34] V. Vapnik and A. Chervonenkis, "On the uniform convergence of relative frequencies of events to their probabilities," *Theory Probab. Appl.*, vol. 16, pp. 264–264, 1971.
[35] V. Vapnik, *Statistical Learning Theory*. New York, NY, USA: Wiley-Interscience, 1998.

Ning Lu (S'12) received the B.Sc. and M.Sc. degrees in electrical engineering from Tongji University, Shanghai, China, in 2007 and 2010, respectively, and is currently pursuing the Ph.D. degree in electrical and computer engineering at the University of Waterloo, Waterloo, ON, Canada.

His current research interests include capacity and delay analysis, real-time scheduling, and cross-layer design for vehicular networks.

Mr. Lu served as a Technical Program Committee Member for the 2012 IEEE International Symposium on Personal, Indoor, and Mobile Radio Communications.

Tom H. Luan received the B.E. degree from Xi'an Jiaotong University, Xi'an, China, in 2004, the M.Phil. degree from the Hong Kong University of Science and Technology, Kowloon, Hong Kong, in 2007, and the Ph.D. degree from the University of Waterloo, Waterloo, ON, Canada, in 2012, all in electrical engineering.

His current research interests focus on wired and wireless multimedia streaming, QoS routing in multihop wireless networks, peer-to-peer streaming, and vehicular network design.

Miao Wang received the B.Sc. degree in electrical engineering from Beijing University of Posts and Telecommunications, Beijing, China, in 2007, and the M.Sc. degree in electrical engineering from Beihang University, Beijing, China, in 2010, and is currently pursuing the Ph.D. degree in electrical and computer engineering at the University of Waterloo, Waterloo, ON, Canada.

Her current research interests include traffic control, capacity and delay analysis, and routing protocol design for vehicular networks.

Xuemin (Sherman) Shen (M'97–SM'02–F'09) received the B.Sc. degree from Dalian Maritime University, Dalian, China, in 1982, and the M.Sc. and Ph.D. degrees from Rutgers University, New Brunswick, NJ, USA, in 1987 and 1990, respectively, all in electrical engineering.

He is a Professor and University Research Chair with the Department of Electrical and Computer Engineering, University of Waterloo, Waterloo, ON, Canada. He was the Associate Chair for Graduate Studies from 2004 to 2008. He is a coauthor/editor of six books and has published many papers and book chapters in wireless communications and networks, control, and filtering. His research focuses on resource management in interconnected wireless/wired networks, wireless network security, wireless body area networks, and vehicular ad hoc and sensor networks.

Dr. Shen is a registered Professional Engineer of Ontario, Canada, a Fellow of the Canadian Academy of Engineering, a Fellow of the Engineering Institute of Canada, and a Distinguished Lecturer of the IEEE Vehicular Technology Society and IEEE Communications Society. He served as the Technical Program Committee Chair for IEEE VTC Fall 2010, the Symposia Chair for IEEE ICC 2010, the Tutorial Chair for IEEE VTC Spring 2011 and IEEE ICC 2008, the Technical Program Committee Chair for IEEE GLOBECOM 2007, the General Co-Chair for Chinacom 2007 and QShine 2006, the Chair for the IEEE Communications Society Technical Committee on Wireless Communications, and P2P Communications and Networking. He also serves/served as the Editor-in-Chief for *IEEE Network*, *Peer-to-Peer Networking and Application*, and *Communications*; a Founding Area Editor for IEEE TRANSACTIONS ON WIRELESS COMMUNICATIONS; an Associate Editor for IEEE TRANSACTIONS ON VEHICULAR TECHNOLOGY, *Computer Networks*, and *Wireless Networks*; and a Guest Editor for the IEEE JOURNAL ON SELECTED AREAS IN COMMUNICATIONS, *IEEE Wireless Communications*, *IEEE Communications Magazine*, and *Mobile Networks and Applications*.

Fan Bai received the B.S. degree in automation engineering from Tsinghua University, Beijing, China, in 1999, and the M.S.E.E. and Ph.D. degrees in electrical engineering from the University of Southern California, Los Angeles, CA, USA, in 2005.

He has been a Senior Researcher with the Electrical and Control Integration Laboratory, Research and Development and Planning, General Motors Corporation, Warren, MI, USA, since 2005. He is also serving as a Ph.D. supervisory committee member with Carnegie Mellon University, Pittsburgh, PA, USA, and the University of Illinois at Urbana–Champaign, Urbana, IL, USA. He has published about 40 book chapters and conference and journal papers, including in ACM MobiCom, IEEE INFOCOM, ACM MobiHoc, IEEE SECON, IEEE ICC, IEEE GLOBECOM, IEEE WCNC, the IEEE JOURNAL ON SELECTED AREAS IN COMMUNICATIONS, *IEEE Wireless Communication Magazine*, *IEEE Communications Magazine*, and *Ad Hoc Networks*. His current research is focused on the discovery of fundamental principles and the analysis and design of protocols/systems for next-generation vehicular ad hoc networks (VANET), for safety, telematics, and infotainment applications.

Dr. Bai is an Associate Editor of the IEEE TRANSACTIONS ON VEHICULAR TECHNOLOGY and IEEE TRANSACTIONS ON MOBILE COMPUTING and serves as a Guest Editor for the *IEEE Wireless Communication Magazine*, *IEEE Vehicular Technology Magazine*, and *Ad Hoc Networks*. He served as a Technical Program Co-Chair for IEEE WiVec 2007 and IEEE MoVeNet 2008. In 2006, he received the Charles L. McCuen Special Achievement Award from General Motors Corporation in recognition of extraordinary accomplishment in the area of vehicle-to-vehicle communications for drive assistance and safety.